Rotating disk electrode to measure diffusivity of metal ions and kinetic parameters in heterogeneous electrochemical reactions

by

Shital Babu Rijal

B.Sc., Tribhuvan University, Nepal, 2014

M.Sc., Sikkim University, India, 2017

A THESIS

submitted in partial fulfillment of the
requirements for the degree

MASTER OF SCIENCE

Department of Physics
College of Arts and Sciences

KANSAS STATE UNIVERSITY
Manhattan, Kansas

2022

Approved by:

Major Professor
Bret N. Flanders

Copyright

© Shital Babu Rijal 2022.

Abstract

Chemical reaction rates are generally amplified by using a catalyst and lowering the reaction energy barrier, or by raising the temperature or pressure of the system to increase reactants' thermal energy. Regarding electrochemical reactions in solutions, we hypothesize that a rapidly changing electric field will enhance the Brownian motion of reactant ions to increase their effective temperature. Hence this technique, termed stochastic heating, is an attractive alternative for reaction rate enhancement. To test this hypothesis, we need to characterize the kinetics of the chemical reaction. Here we use a rotating disk electrode to measure the kinetic parameters and diffusivity of metal ions in the following electrochemical systems. We present a self-verifiable procedure to measure the heterogeneous rate constant of ferrous/ferric ions at the platinum electrode and their diffusivity in the chloride system. We determine favorable supporting electrolytes for studying silver and indium ions and for characterizing their kinetics. The quantities thus measured are trustworthy bases for comparing with modified systems to enhance the reaction rate in the presence of stochastic noise.

Table of Contents

List of Figures vii

List of Tables ix

Acknowledgements x

Dedication xi

1 Introduction 1

2 Theory 6

2.1 Kinetic parameters of electrochemical reactions 6

2.2 The exchange current 8

2.3 Electrochemical layers and diffusivity 10

2.4 Three-electrode electrolytic cell 12

2.5 Voltammetry 14

2.5.1 Cyclic Voltammetry 14

2.5.2 Linear voltammetry 15

2.6 Limitations in measurement of kinetic parameters 16

2.7 Rotating disk electrode 17

2.8 Levich analysis 18

2.9 Butler-Volmer equation 20

2.10 Koutecky-Levich analysis 22

2.11 Tafel analysis 23

3 Diffusivity and kinetic parameters of ferrous/ferric redox reaction in chloride medium 25
3.1 Introduction . . . 25
3.2 Experimental . . . 26
3.3 Analysis . . . 29
3.3.1 Levich Analysis . . . 29
3.3.2 Koutecky-Levich Analysis . . . 31
3.3.3 Tafel Analysis . . . 33
3.3.4 Linearity at low overpotentials . . . 34
3.4 Results and conclusion . . . 35

4 Diffusivity and kinetic Parameters of silver ions in perchlorate medium . . . 37
4.1 Introduction . . . 37
4.2 Experimental . . . 38
4.3 Analysis . . . 40
4.3.1 Levich Analysis . . . 40
4.3.2 Koutecky-Levich Analysis . . . 42
4.3.3 Tafel Analysis . . . 43
4.4 Results and conclusion . . . 44

5 Development of appropriate system to measure diffusivity of indium ions in acetate medium . . . 45
5.1 Introduction . . . 45
5.2 Experimental . . . 46
5.3 Analysis . . . 52
5.3.1 Levich Analysis . . . 52
5.4 Results and conclusion . . . 54

6 Conclusion and future prospects . . . 55

Bibliography 58

A Python code to run electrode rotator, take CV and take LSV for Indium system . 62

List of Figures

2.1 Energy barrier diagram at equilibrium 6

2.2 Energy barrier diagram at a potential $E < E_0$ 7

2.3 Electrochemical layers outside an electrode 10

2.4 Variation of concentration and momentum outside an electrode 11

2.5 Schematic diagram for a basic potentiostat 13

2.6 Cyclic Voltammogram (CV) 14

2.7 Linear Sweep Voltammogram (LSV) 15

2.8 Linear Sweep Voltammogram (LSV) regions 16

2.9 Rotating Disk Electrode setup 17

2.10 Rotating Disk Electrode 18

2.11 Levich plot 19

2.12 Linearity of current at low overpotentials 21

2.13 Koutecky-Levich plot 23

2.14 Tafel plot 24

3.1 CV for iron system 28

3.2 CV for iron system at different rotation speeds 29

3.3 Levich plot for iron 30

3.4 Koutecky-Levich plot for ferrous oxidation 31

3.5 Koutecky-Levich plot for ferric reduction 32

3.6 Tafel plot for iron system 33

3.7 Low overpotential approximation to measure i_0 34

4.1 CV for silver system 39

4.2 LSV for silver at different rotation speeds 40
4.3 Levich plot for silver 41
4.4 Koutecky-Levich plot for silver ion reduction 42
4.5 Tafel plot for silver 43

5.1 CV for indium system - I 47
5.2 LSV for indium system at different rotation speeds - I 48
5.3 CV and LSV for indium system - II 49
5.4 Background current in the indium system 50
5.5 CV and LSV for indium system - III 51
5.6 LSV for indium system - IV 52
5.7 Levich plot for indium system 53

List of Tables

3.1 Measurement of slope, and calculation using Equation 2.33 for i_0, and Equation 2.11 for j_0 and k_0. 35

Acknowledgments

First of all, I want to express my sincere gratitude to my research supervisor Prof. Bret N. Flanders. He set challenges in front of me, and made me believe I can achieve those. I have found myself to have developed lots of skills and talents under his guidance. Huge shout out to Krishna Pant who is more than a lab-mate. He guided and helped me settle in the lab in my early days and is doing until now. I thank the other members of my research group, Christine Orme and Xiaoxie Xu from Lawrence Livermore National Lab, for their insightful suggestions. I thank Prof. Bruce M. Law who was my first supervisor at K-State and taught me how to perform experiments to obtain precision and accuracy. I am thankful to Prof. Mathew Berg and Prof. Jeremy Schmit for being a part of my supervisory committee. Their insights and suggestions are valuable to my progress.

I am thankful to my teachers in Department of Physics, KSU, for theory courses which have contributed in some way to this thesis. Thanks to Prof. Mick O'Shea for advising me throughout my graduate studies, and Kim Coy for being there and taking care of us. Other staffs of the department, Kim Elliott, Cindy Carlyon, Kelsey Young and Austin Roberts, I am equally thankful to them for their immediate response and help in logistics.

I am thankful to the Nepalese community in Manhattan, Kansas who made this place feel like home. I am always grateful to Prof. Archana Tiwari for being my first physics mentor at Sikkim University, India. Special thanks to my family - parents, grandparents and in-laws in Nepal, my brother and my sister in Australia, and my wife Parikshya and son Parixit, who have always given me a motivation to work harder.

At the end, thanks to Keck foundation for supporting this project and my entire research that this thesis is based on.

Dedication

To my wife Parikshya and son Parixit

Chapter 1

Introduction

In heterogeneous chemical reactions, the reactants are in two or more different phases, or the reactants change phase after the reaction. Electrolytic and galvanic cells are examples of heterogenous electrochemical reactions where the ions in electrolytic solution interact with the solid electrodes. And the efficiency and performance of the modern world devices based on chemical reactions can be improved by ultrafast electrochemistry and enhanced reaction rate. So, the characterization of heterogeneous chemical reactions that govern such systems, by a higher accuracy is more important than ever. Thus, we have worked on improving a procedure and method to accurately and precisely measure the kinetic parameters of heterogeneous chemical reactions.

The diffusivity, D, takes part in the transfer rate of ions from the bulk electrolytic solution to the electrode surface which is the first step of the reaction. And the standard heterogeneous reaction rate constant, k_0, gives the measure of the tendency of ions to donate or receive electrons to and from the electrodes once they reach the electrode surface, which is the second step.

This research focuses particularly on electrochemical reactions between a metal electrode and ions in an electrolytic solution. The main objectives are listed below:

- Measuring the diffusivity of ions – iron, silver, and indium in an electrolytic solution
- Measuring the heterogenous rate constant and transfer coefficient for ferrous and ferric

ions in chloride electrolytic medium

- Measuring the heterogenous rate constant and transfer coefficient for silver ions in perchlorate electrolytic medium

In an electrolytic system, the reaction occurs in two-halves, oxidation half - where an ion loses an electron to oxidize, and reduction half - where an ion gains an electron to reduce. As the first step, an oxidation or reduction process requires that the ions travel from bulk solution to the reaction site - the electrode surface. This may happen by three processes - migration, diffusion, and convection. Migration refers to the travel of ions due to force by an electric field, which does not happen here because of shielding effect of the electrolytes. Diffusion is due to the concentration gradient across the bulk and the electrode surface. Convection happens due to mechanical force on the ions such as the hydrodynamic force due to stirring of solution or rotation of electrode. As a second step, the ions should have enough energy to cross the energy barrier for reaction which includes desolvation, crossing the electric double layer, finding a reaction site in electrode, exchanging the electron, and finally, either settling on the electrode or returning back to the electrolytic solution. This required energy is externally provided by the potential of the electrode.

When the reaction occurs, initially there is enough mass of ions near the electrode surface that is available to react. The mass that reacts creates a lower concentration of ions near the electrode and that is fulfilled by diffusion of ions from the bulk. As long as the diffusion is sufficient to supply enough ions for reaction, electric current following through such reactions is dependent on how fast the electron transfer process between the ions and the electrode can take place. Such a reaction is called kinetic limited reaction and current is called kinetic limited current or simply kinetic current, i_k.

At higher potential (or lower potential depending upon the ion polarity), the reaction happens so fast that the diffusion lags behind to provide enough ions near the electrode surface. Reaction reaches to a steady state whose rate is completely a function of diffusion and the electric current following through the system is constant. Such a reaction is called diffusion-limited reaction and the current is called diffusion-limited current.

A part of our objective is to measure the diffusivity of such ions. The diffusivity of ions depends on several factors mainly the temperature, and the viscosity of the solution it is present in. The impracticality to create a comprehensive table of diffusivity values makes it necessary to develop an easy technique to measure the diffusivity for any customized experimental condition. To measure diffusivity, it is important to take the reaction to diffusion-limited state. But to measure the kinetics, we do not want diffusivity to limit the reaction. We want a technique which can separate to some extent, the kinetic limited region and diffusion-limited region. That allows us to play on the kinetic limited region to measure the kinetic parameters and on the diffusion-limited region to measure the diffusivity. And a technique that can help accomplish this task is Rotating Disk Electrode (RDE).

In RDE technique, convection helps transfer mass towards the electrodes so that an ample amount of mass reaches to the electrode. With this, the mass transfer does not limit the reaction so early and in that region, the reaction is totally dependent on chemical kinetics. We study that region to measure the kinetic parameters of the chemical reaction. Farther beyond as we reach to the diffusion-limited region, we observe the diffusion-limited reactions at different rotation speeds. That gives us the measure of diffusivity of ions.

RDE technique has developed over time with a spark in 1904 by W. Nernst who for the first time indicated that the reaction rates in heterogeneous chemical reactions can be traced back to the diffusion rates[1]. He showed that a thin layer of fluid close to the electrode and the ions inside that layer always stay at rest with respect to the electrode which he called the diffusion layer. Across this layer, the concentration of ions drops sharply and linearly, from bulk concentration value to zero causing diffusion.

When it was established that diffusion can limit the current to a maximum value, called limiting current, several experiments were done to figure out what factors the limiting current could depend upon. The diffusion and diffusivity were of primary interest. Nernst and Merriam in 1905 through their paper - On the theory of residual current, established the direct proportionality between the limiting current and the concentration of the solution[2].

Eucken in 1932 did an experiment to show that the limiting current is proportional to the revolving speed of the electrode to the power 0.5-0.6 and the diffusivity to the power

$2/3$[3].

The credit to a complete solution to the mass transfer problem goes to Benjamin Levich[4]. His approach was based on modern theories of fluid mechanics. He coupled the general equation for diffusion, convection, and migration, with the Navier-stokes equation for fluid motion. He considered the Poisson equation for the charge distribution to obtain a complete theory of concentration polarization in the region near the electrode. He established the existence of two different layers – diffusion layer and hydrodynamic boundary layer. The hydrodynamic layer is the one up to which the fluid is dragged by the electrode. The diffusion layer lies nearer to the electrode inside which concentration drops sharply from bulk concentration to zero and diffusivity plays a role. Through his book, physicochemical hydrodynamics[5] in 1962, he derived the thickness of the diffusion boundary layer which depended on the diffusivity of the ions, viscosity of electrolytic solution and rotation speed of the electrode, shown later in Equation 2.26. In the same book, he established the general equation for diffusion-limited current which is known as the Levich Equation. Jaroslav Koutecky and Levich[6] in 1958, worked together to study the transport and kinetics in catalytic processes and established the relation between diffusion-limited current with kinetic current which is famously known as Koutecky-Levich equation. Rotating Disk Electrode analysis uses the above two equations in particular to give us the values of diffusivity and kinetic parameters. We call that Levich anlysis and Koutecky-Levich analysis.

The reason behind our objectives basically is to study the enhancement in rate of chemical reactions in the kinetic region by using stochastic noise signal. We hypothesize that the random motion of ions close to the electrode due to the effect of electric force created by the stochastic noise imitates the Brownian motion, and hence increases their effective temperature. This should increase the rate at which the reaction occurs and standard heterogeneous rate constant is the parameter that reflects this increased rate if any. So, we needed to establish a trustworthy and precise method to measure the kinetics using Rotating Disk Electrode. Since the diffusivity also plays a role in the overall chemical reaction rate, we also wanted to measure the diffusivity of ions in different electrolytic media.

For our study, we have chosen three different types of systems - iron system, where two

species of ions are present in the system that change into one another at the electrode surface but do not deposit and remain within the solution; Silver system with only one ion species in the solution but has real deposition on the electrode and can be cleaned electrochemically; And finally indium system which is similar to silver system except that it can't be cleaned electrochemically. We have chosen to work on less studied electrolytic media to provide a better scope for our experiments.

We have worked on the minute details of system preparation to achieve better measurements. We have used two different techniques to acquire the current-potential information - one using the commercially available potentiostat and software, and the other using a self made potentiostat and python programming that reduces the cost and permits customization of the electronics. We have verified our results with literature values and concluded on a satisfactory note that our procedure and results are good bases for further studies.

Chapter 2

Theory

2.1 Kinetic parameters of electrochemical reactions

In an electrochemical reaction, the parameters that play a role in the kinetics are the transfer coefficient α and the standard heterogeneous rate constant k_0. Consider a one-electron redox reaction between an oxidant, O, and reductant, R.

$$O + e \underset{k_b}{\overset{k_f}{\rightleftharpoons}} R$$

where, e is the electronic charge, k_f is the forward rate constant and k_b is the backward rate constant.

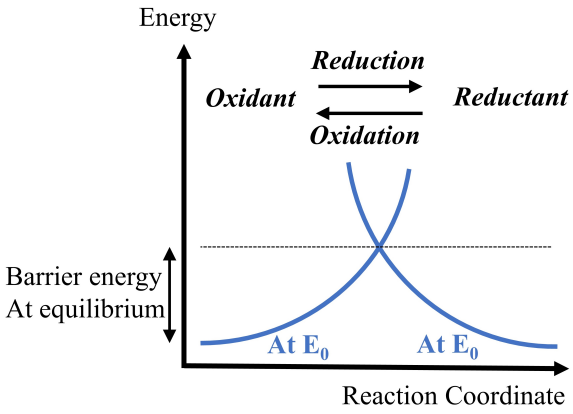


Figure 2.1: *Energy barrier diagram at equilibrium*

In the forward reaction, the oxidant gains an electron and gets reduced, while in the backward reaction, the reductant loses an electron and gets oxidized, jointly called a redox reaction. The heterogeneous rate constant k_0 refers to the rate at the time when this redox reaction is in equilibrium. In that state, the reduction (forward) rate constant, k_f and the oxidation (backward) rate constant, k_b are equal. Arrhenius was the first to generalize the chemical reaction rate and proposed the Arrhenius law,

$$k = Ae^{\frac{-EnergyBarrier}{RT}}, \tag{2.1}$$

where, k is the rate constant which could be forward or backward, unit – $cm\ s^{-1}$;
T is the temperature, unit – K;
R is the universal gas constant, unit – $J\ mol^{-1}\ K^{-1}$;
A is generally called the frequency factor, unit – $cm\ s^{-1}$.

We are looking at the electrochemical reaction between a metal electrode and ions inside an electrolytic solution. The metal which is kept at a certain potential with respect to the ground takes part in the reaction with the ions. At a certain electric potential with respect to a reference electrode, the reduction and oxidation rates of ions onto the electrode are equal. This voltage is called the equilibrium potential and denoted by E_0.

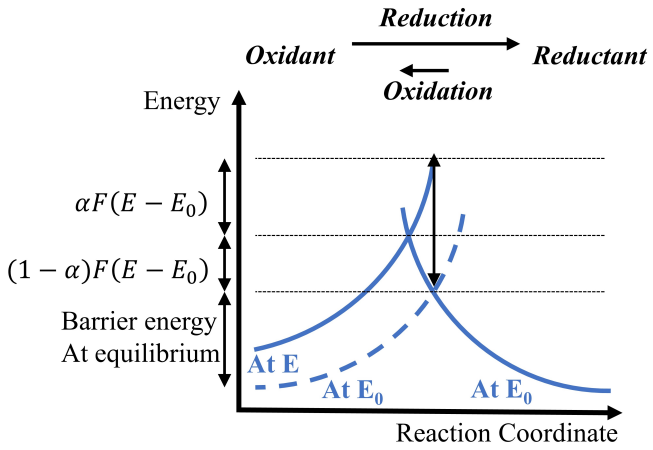


Figure 2.2: *Energy barrier diagram at a potential $E < E_0$*

When the potential is away from the equilibrium potential, suppose, at $E < E_0$, the

symmetry between the energy curves between the forward and backward reaction breaks. The relative energy of electron on the electrode surface changes by $-F(E - E_0)$, hence the $O + e$ curve moves up by this quantity. The barrier for oxidation then increases by a fraction of that amount, $(1-\alpha)$ where α is called the transfer coefficient or sometimes called the symmetry factor since it represents the symmetry of the forward and backward energy curves.

Under such a potential, the forward and the backward reaction rates are not equal and now denoted by k_f and k_b respectively, and given by,

$$k_f = k_0 e^{-\frac{\alpha F(E-E_0)}{RT}}, \tag{2.2}$$

$$k_b = k_0 e^{\frac{(1-\alpha)F(E-E_0))}{RT}}. \tag{2.3}$$

At $E = E_0$, k_f is equal to k_b and are both k_0 which is called the standard heterogeneous rate constant, and the key parameter for us to measure.

2.2 The exchange current

Consider an electrode of surface area A in a solution of concentration C. The rate at which reaction takes place at the electrode, v $(mol\ s^{-1})$ is proportional to C and A, k being the proportionality constant,

$$v = kAC. \tag{2.4}$$

In terms of number of moles N of ions reacting with the electrode, v can be also written as,

$$v = \frac{dN}{dt}. \tag{2.5}$$

Current and charge produced by the above reaction can be written as,

$$\frac{dN}{dt} = \frac{d(\frac{Q}{nF})}{dt} = \frac{i}{nF}, \tag{2.6}$$

where, i is the current, Q is the charge, n is the number of electrons exchanged, t is the time and F is the Faraday constant – 96500 $C\ mol^{-1}$.

Referring to Equations 2.4, 2.5 and 2.6, we can get to this equation for current,

$$i = nkFAC. \tag{2.7}$$

The current due to reduction or the forward reaction is called the cathodic current,

$$i_c = nk_fFAC_O(0) \tag{2.8}$$

where, k_f is the forward reaction rate constant, and $C_O(0)$ is the concentration of the oxidant species at the electrode surface, where Z = 0.

In the same way, the current due to oxidation or the backward reaction is called the anodic current,

$$i_a = nk_bFAC_R(0), \tag{2.9}$$

where, k_b is the backward reaction rate constant, and $C_R(0)$ is the concentration of the reductant species at the electrode surface.

The overall current would then be,

$$i = i_c - i_a = nFA(k_fC_O(0) - k_bC_R(0)). \tag{2.10}$$

At equilibrium, the net current is zero and the concentration at the surface $C(0)$ is equal to that of the bulk C for both the oxidant and reductant species,

$$i_c = i_a = i_0 = nk_0FAC. \tag{2.11}$$

Here, i_0 is called the exchange current, and $j_0 = \frac{i_0}{A} = nk_0FC$ is called the exchange current density.

2.3 Electrochemical layers and diffusivity

We are interested in heterogeneous electrochemical reactions between metal ions and metal electrodes. The schematic figure below shows hydrated positive ions in an aqueous solution.

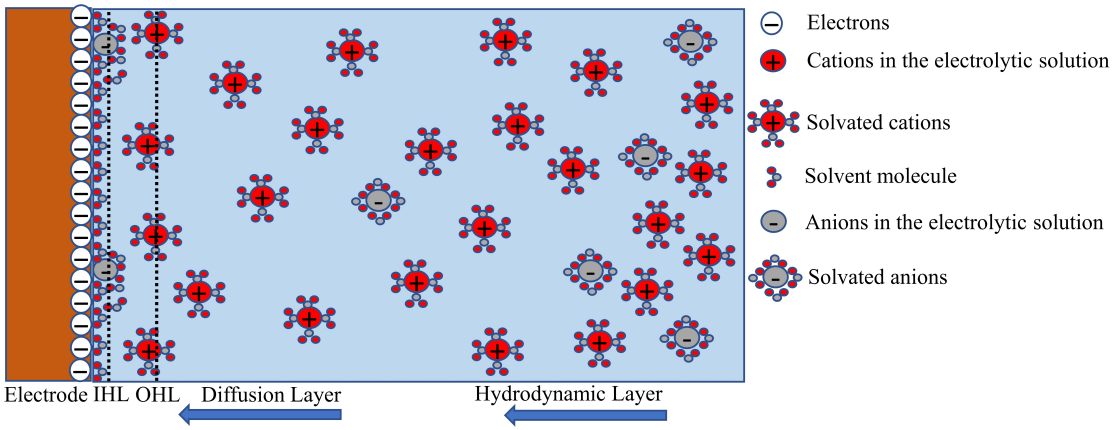


Figure 2.3: *Electrochemical layers outside an electrode placed on an electrolytic solution*

The metal electrode is kept at a negative potential. The Helmholtz model provides a simple approximation to screening layers that exist closest to an electrode. The Inner Helmholtz Layer (IHL) is comprised of solvent molecules and specifically adsorbed ions in direct contact with the metal surface. Outer Helmholtz Layer (OHL) is the layer beyond which we can find the solvated ions. Together these two planes facilitate the electron transfer to and from the electrode surface to drive electrochemical redox reactions. The size of this double layer can be approximated by the Debye length,

$$\kappa^{-1} = \sqrt{\frac{\epsilon_r \epsilon_0 k_B T}{2Cn^2e^2}}, \tag{2.12}$$

where, T is temperature, k_B is Boltzmann's constant, and e is the electronic charge.

Beyond the electric double layer, lies the diffusion layer. Concentration gradient across this layer and the bulk is maximum. This influences the spontaneous movement of ions from the high concentration region (bulk) to the region of lower concentration (diffusion layer) to minimize the concentration difference. Such a phenomenon is called diffusion.

The diffusion layer thickness is arbitrary due to the asymptomatic change in concentra-

tion. It depends on the diffusivity, D. In an electrochemical study, the rate of change of potential of the electrode, called the scan rate, also affects the diffusion layer thickness. At slow scan rates, the diffusion layer is large, in order of micrometers, whereas at fast scan rates the diffusion layer is nanometers in thickness.

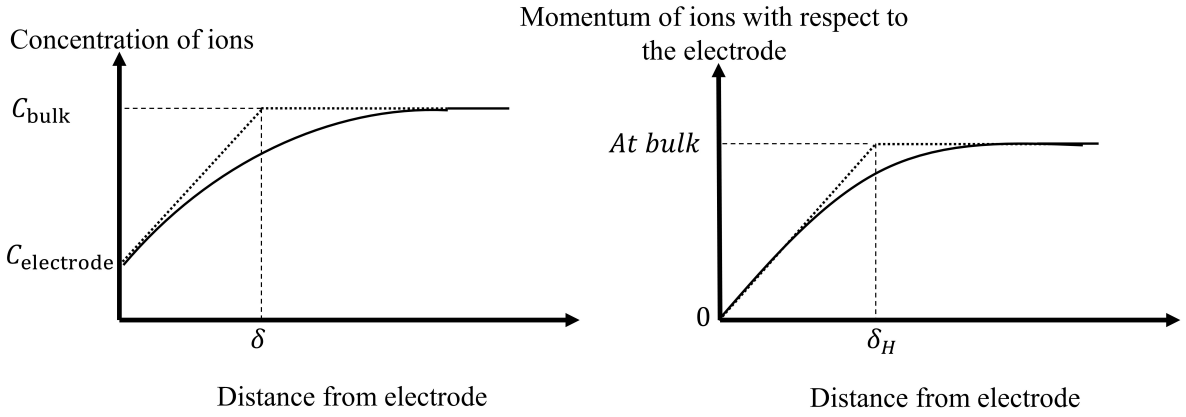


Figure 2.4: *Variation of concentration of ions, and momentum of ions with respect to the momentum of electrode*

To introduce diffusivity, we use the semi-empirical treatment of the steady-state mass transfer. Flux is proportional to the concentration gradient at the electrode surface with proportionality constant - Diffusivity.

$$J_D = -D\left(\frac{dC}{dz}\right)_{z=0}, \tag{2.13}$$

which is also called the Fick's first law. Consider a linear concentration gradient within the diffusion layer,

$$J_D = -D\frac{(C - C(0))}{\delta}, \tag{2.14}$$

where δ is the diffusion layer thickness. Current due to the diffusive flux is

$$i = -nFAJ_D = nFAD\left(\frac{dC}{dz}\right)_{z=0} = nFAD\frac{(C - C(0))}{\delta}. \tag{2.15}$$

Current is limited by diffusion in case when the concentration on the electrode surface, $C(0) = 0$. So, $C - C(0) \approx C$.

This diffusion-limited current is,

$$i_l = nFAD\frac{C}{\delta}. \tag{2.16}$$

Rearranging the terms in Equations 2.15 and 2.16 for total current and limited current allows us to derive relation between the limited current and total current,

$$\frac{C(0)}{C} = 1 - \frac{i}{i_l}. \tag{2.17}$$

Beyond the diffusion layer lies the hydrodynamic layer. It is considered to be the region up to where the liquid is dragged by a moving surface, such as a rotating electrode. This is the region where the momentum of ions sharply decreases from that at bulk to zero at electrode. For a disk rotating at speed, ω, in a solution of kinematic viscosity, ν, hydrodynamic boundary layer is related to the diffusion boundary layer by the following equation,

$$\delta_H \approx 2\left(\frac{\nu}{D}\right)^{\frac{1}{3}}\delta. \tag{2.18}$$

And in terms of ω and ν is,

$$\delta_H \approx 3\left(\frac{\nu}{\omega}\right)^{\frac{1}{2}}. \tag{2.19}$$

2.4 Three-electrode electrolytic cell

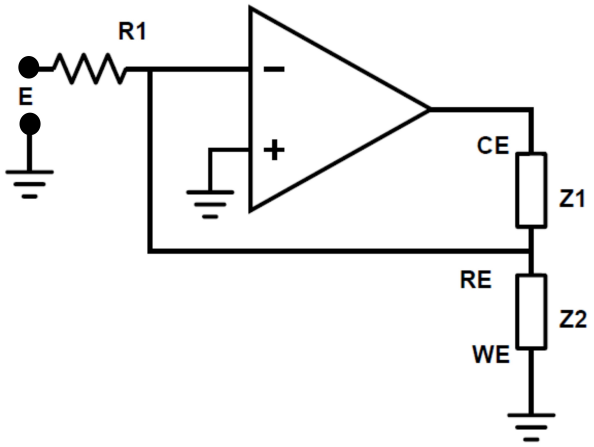
The basic idea in studying electrochemistry is changing the potential of an electrode of interest to induce a chemical reaction of interest to observe the current that follows. That electrode is called the working electrode (WE). A second electrode is used to create a potential difference inside the electrolyte. In such a two-electrode cell, when we supply the potential difference across the electrodes, an electric potential difference is developed across electric double layer at the electrode-electrolyte interface. This electric potential difference does not have a fixed value and changes as the current flows. This prohibits us to say exactly, what the potential of the working electrode is. In addition, any change in the supplied electric potential may not be equal to the potential difference across the interface. Thus

comes the need of a 3-electrode cell.

In a 3-electrode cell, a third electrode called the reference electrode (RE) is used as a probe to better define the potential drop across the working electrode interface. An RE is a special kind of electrode, or a combination of electrode and electrolyte as a system, whose own interfacial potential difference remains fixed, so any change in potential difference between the working and the reference electrode corresponds to the change in the potential difference across the working electrode interface. Some of the common reference electrodes used are, Ag/AgCl, and Saturated Calomel Electrode (SCE).

To balance the oxidation or reduction at the working electrode, the ions of opposite polarity need a reaction site. For that, a third electrode is used which is called the counter electrode (CE) or auxillary electrode (AE). It helps supply or receive the current to or from the system according to the reactions occuring at the working electrode. These three electrodes - WE, RE and CE inside an electrolytic solution constitute the electrochemical system.

A potentiostat is used to control the potential of the working electrode and measure the current flowing across the system. A schematic diagram is shown below.



$$V_{RE} = \frac{1}{1 + (\beta A)^{-1}} E,$$

where,

$$\beta = \frac{Z1}{Z1 + Z2} \text{ and } A = \text{open loop gain}$$

Figure 2.5: *Schematic diagram for a basic potentiostat*

When current flows across the system, the potential difference across the electrode-electrolyte interface of the working electrode changes. The change is fed back to the control amplifier. To counter the change and to keep the potential fixed at E, the control amplifier

flows in or draws out the necessary current and maintains the reference electrode at the supplied potential.

2.5 Voltammetry

Voltammetry is a method of studying an analyte by observing its behavior, or current in the electrolytic systems, as a function of potential. The results from voltammetry are obtained in the form of IV curves which are called voltammograms. For voltammetry, the potential is varied continuously or step by step with time. Different types of voltammetry are cyclic, linear sweep, square wave, stripping, alternating current, pulse, steady-state microelectrode, and hydrodynamic voltammetry. Of these several useful techniques of voltammetry two are used for this study – Cyclic and Linear.

2.5.1 Cyclic Voltammetry

Cyclic voltammetry is a reversal technique of applying voltage. A starting potential is selected, usually one of the extreme voltages at which full phased oxidation or reduction occurs. Suppose we select and supply extreme positive side potential, E_1 where oxidation

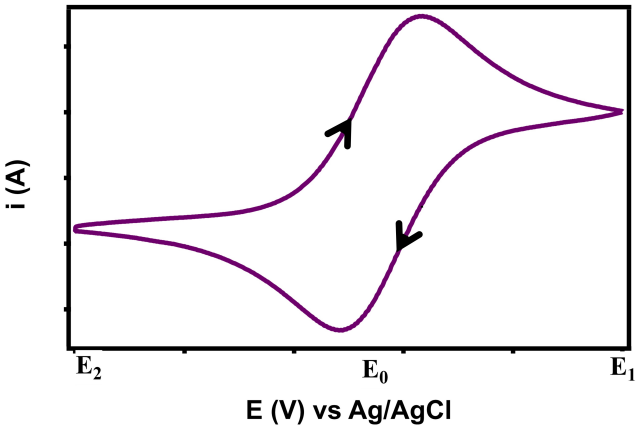


Figure 2.6: *Cyclic Voltammogram run for a system along E_1, E_0, E_2 and reversed back*

occurs. Potential is then swept along the equilibrium potential, E_0 towards the extreme

negative side potential, E_2, where reduction occurs. Then the potential is reverse backed from E_2 along E_0 to E_1. This constitutes one cycle and can be repeated multiple times to get a reproducible IV cyclic curve which is called the cyclic voltammogram (CV). An example of a CV for Ferrous-Ferric system is shown in Figure 2.6. The current stops increasing after the peaks on both reduction and oxidation regions, because of the limitation in mass availability by diffusion, which will be discussed later in detail in Section 2.6

2.5.2 Linear voltammetry

Linear sweep voltammetry (LSV) is the breakdown of a cyclic voltammetry where the scan is done only along either the reduction or oxidation side. There is no reversal of the voltage. This saves our task when we are interested in either reduction or oxidation only, or for an electrolytic solution, that has only one of the species, either oxidant or reductant. An example of an LSV for reduction of silver ions is shown below.

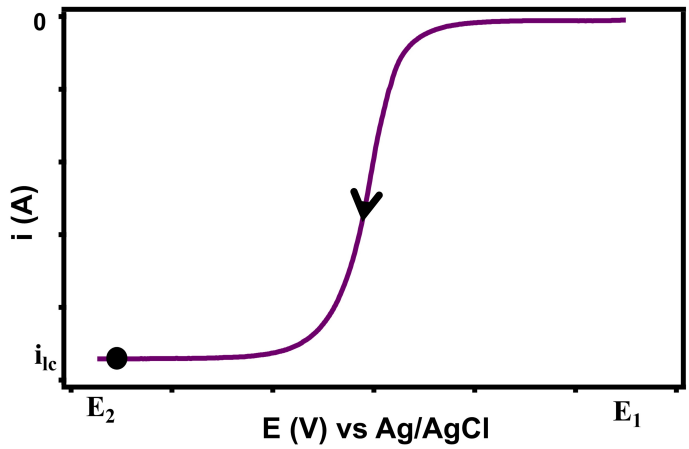


Figure 2.7: *Linear sweep voltammogram taken with a rotating disk electrode (100 RPM) starting from E_1 and ending to E_2,*

2.6 Limitations in measurement of kinetic parameters

The basic idea is to sweep E and look at the variation of i with E and ultimately k_f with E to obtain k_0 and α.

$$i_c = nk_f FAC_O \tag{2.20}$$

$$k_f = k_0 e^{-\frac{\alpha F(E-E_0)}{RT}} \tag{2.21}$$

When reduction just starts to begin, shown by the increased negative current, there is

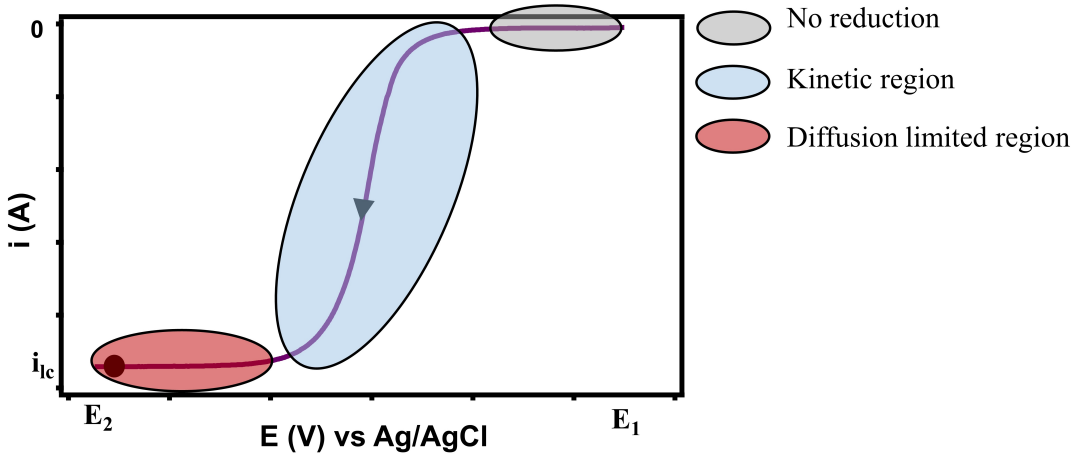


Figure 2.8: *Different regions of an LSV taken for reduction an ion*

enough mass of ions to reduce. Hence, the negative current keeps on increasing as we lower the potential. This is the kinetic region where there is no effect of mass limitation. After a certain period, the current becomes stable and is not affected by further lowering of the potential. This extreme cathodic region towards E_2 where the current is constant, is called the diffusion-limited region, and constant current is the diffusion-limited cathodic current, i_{lc}.

To learn the kinetics of the reaction, the focus should be on the kinetic region of the curve. But as shown in the LSV in Figure 2.8, as we move towards more negative side, the current gets limited by diffusion. The diffusion-limited current is used to measure the diffusivity of the ions but will adversely affect the kinetic measurements. In addition, very

close to equilibirum, significant anodic current is also present which means the current we measure is not purely cathodic. Thus we need a region where the reverse reaction as well as the diffusion-limited reaction minimally affect the current. For that a rotating disk electrode is used that extends the kinetic region of the IV curve.

2.7 Rotating disk electrode

When the current is limited by diffusion, we won't have enough space to work on the kinetic region. So, a Rotating Disk Electrode (RDE) plays a role by delaying the onset of diffusion-limited region. How it does is based on the hydrodynamics. A rotating electrode decreases the diffusion layer thickness outside the electrode, discussed later in Equation 2.26. With that, relatively a larger amount of mass will be available for diffusion and thus for reaction. The dependency of diffusion layer thickness on the rotation speed and other properties of the solution was quantitatively and extensively established by Levich in 1953, which is discussed in the following sections.

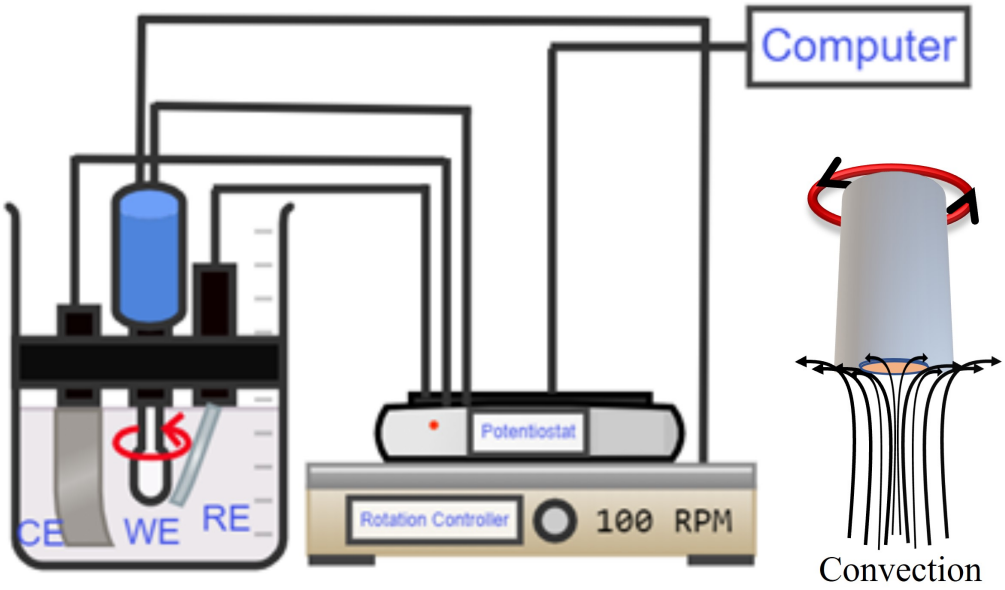


Figure 2.9: *Schematic diagram showing Rotating Disk Electrode setup used in a three electrode setup with a potentiostat*

2.8 Levich analysis

Levich solved the convective-diffusion equation for a rotating disk electrode,

$$\frac{\partial C_j}{\partial t} = D_j \nabla^2 C_j - v_j \nabla C_j, \tag{2.22}$$

to establish the relation between the ion-concentration gradient between the electrode and the bulk. Here, j represents one of the three dimensions considering the disk center as the origin. The term $\frac{\partial C_j}{\partial t}$ represents the variation of concentration of ions on the electrode surface with time, which is zero when the convection reaches to a steady state for a fixed rotation speed. The term $D_j \nabla^2 C_j$ is the contribution due to diffusion, and $v_j \nabla C_j$ is the contribution due to convection.

He used the study done by Von Karman and Cochran[7] on velocity profile of fluid near $(z << (\frac{\nu}{\omega})^{\frac{1}{2}})$ a rotating disk, where ω is the rotation speed and ν is the kinematic viscosity of the solution.

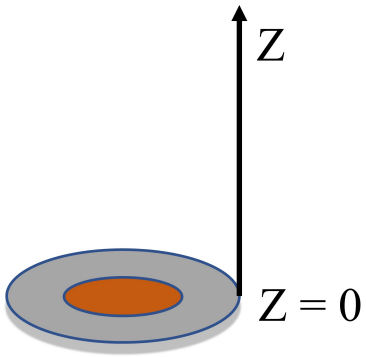


Figure 2.10: *Rotating Disk Electrode*

The boundary equation $C_{z=0} = 0$ applies to the case of current limitation due to absence of ions at the electrode surface. As a solution to the convective-diffusion equation, he derived,

$$\left(\frac{\partial C(z)}{\partial z}\right)_{z=0} = 0.62 D^{-\frac{1}{3}} \omega^{\frac{1}{2}} \nu^{-\frac{1}{6}} C \tag{2.23}$$

From the expression for diffusion-limited current Equation 2.15,

$$i_l = nFAD\left(\frac{\partial C(z)}{\partial z}\right)_{z=0}, \tag{2.24}$$

$$i_l = 0.62nFAD^{\frac{2}{3}}\omega^{\frac{1}{2}}\nu^{-\frac{1}{6}}C. \tag{2.25}$$

This is a comprehensive expression for diffusion-limited current in a rotating disk electrode rotated with angular speed ω, famously known as Levich equation. This equation predicts that i_l is proportional to $\omega^{\frac{1}{2}}$ and C with the proportionality constant $0.62nFAD^{\frac{2}{3}}\nu^{-\frac{1}{6}}$ which is called Levich Constant.

For a constant concentration of ions C, plotting i_l vs $\omega^{\frac{1}{2}}$ should give a straight line passing through the origin which is called the Levich Plot, shown in Figure 2.11 . The slope of the line thus obtained can be used to measure diffusivity.

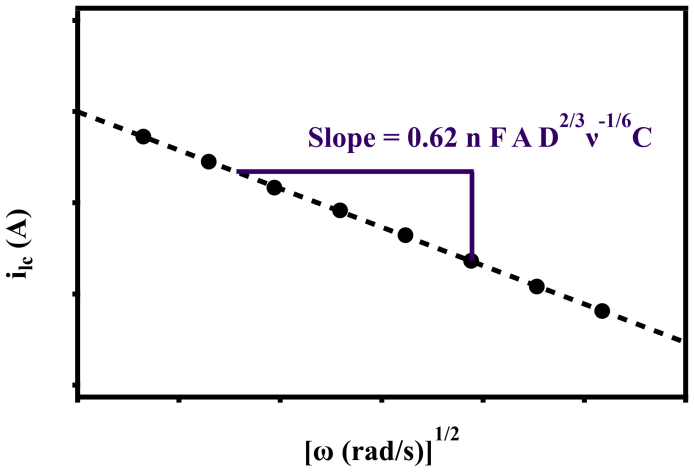


Figure 2.11: *Levich plot showing linear relationship between i_l and ω^{frac12} and passing through the origin. The slope is used to measure diffusivity.*

Comparing with the expression for limiting current, equation 2.16, $i_l = nFAD\frac{C}{\delta}$, we can deduce that diffusion layer thickness is,

$$\delta = 1.61D^{\frac{1}{3}}\nu^{\frac{1}{6}}\omega^{-\frac{1}{2}} \tag{2.26}$$

The validity of Levich equation is subject to a fixed range of rotation speed of the disk[8].

At low values of ω, when the hydrodynamic boundary layer is larger than the disk radius r, the treatment by Von Karman and Cochran for the velocity profiles is not valid. And consequently, Levich equation no longer holds. The lower limit for ω therefore is,

$$\omega > \frac{9\nu}{r^2} \tag{2.27}$$

At large values of ω, laminar flow is overcome by turbulent flow, which occurs at a critical Reynolds number - 2×10^5. And yet again the Levich equation no longer holds. The upper limit for ω is,

$$\omega < \frac{2 \times 10^5 \nu}{r^2} \tag{2.28}$$

2.9 Butler-Volmer equation

Referring to the Equation 2.10 for net current flowing through the system, and Equations 2.2 and 2.3 for rate constants,

$$i = nFAk_0(C_O(0)e^{-\alpha\frac{F}{RT}(E-E_0)} - C_R(0)e^{(1-\alpha)\frac{F}{RT}(E-E_0)}). \tag{2.29}$$

This expression of current is broadly known as Butler-Volmer equation. The other equations further derived as special cases of this equation are used in treatment of almost every problem that involves heterogeneous kinetics.

Using expression from Equation 2.17 for $C_O(0)$ and $C_R(0)$,

$$i = nFAk_0\left(C_O\left(1-\frac{i}{i_{lc}}\right)e^{-\alpha\frac{F}{RT}(E-E_0)} - C_R\left(1-\frac{i}{i_{la}}\right)e^{(1-\alpha)\frac{F}{RT}(E-E_0)}\right). \tag{2.30}$$

In case of equal concentration of oxidant and reductant species in the bulk, $C_O = C_R = C$,

$$i = nFAk_0C\left(\left(1-\frac{i}{i_{lc}}\right)e^{-\alpha\frac{F}{RT}(E-E_0)} - \left(1-\frac{i}{i_{la}}\right)e^{(1-\alpha)\frac{F}{RT}(E-E_0)}\right). \tag{2.31}$$

Substituting the expression from Equation 2.11 for i_0,

$$i = i_0 \left(\left(1 - \frac{i}{i_{lc}} \right) e^{-\alpha \frac{F}{RT}(E-E_0)} - \left(1 - \frac{i}{i_{la}} \right) e^{(1-\alpha)\frac{F}{RT}(E-E_0)} \right) \tag{2.32}$$

This is a special case of Butler-Volmer equation, that includes exchange current, i_0 and the diffusion-limited currents i_l.

At region very close to the equilibrium potential, i.e., $E \approx E_0$, Taylor expanding the exponential term with the condition, $\frac{F}{RT}(E - E_0) << 1$,

$$E - E_0 = i \frac{RT}{F} \left(\frac{1}{i_0} + \frac{1}{i_{lc}} - \frac{1}{i_{la}} \right) \tag{2.33}$$

This equation implies that at the region very near to the equilibrium potential, the E vs i plot is a straight line, and the slope gives us the value of i_0, given that we know i_{lc} and i_{la}. And using the value of i_0, we can find the value of k_0. This is another method to determine or verify the heterogeneous rate constant but is not useful to find α. A schematic diagram is shown in figure 2.13.

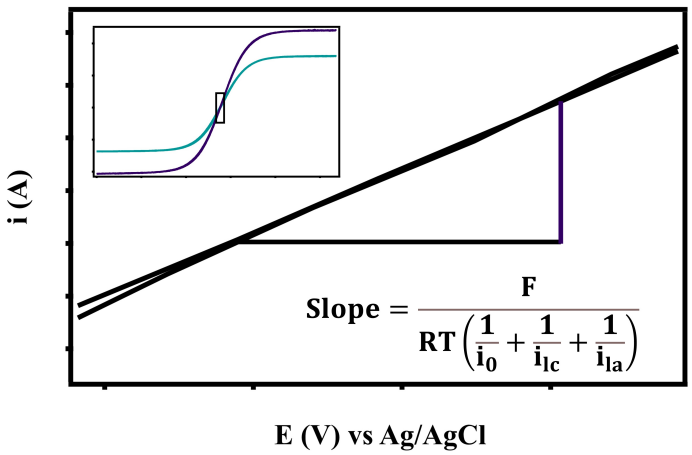


Figure 2.12: *Linearity of current at extremely low overpotentials. The slope of such a trace can be used to calculate i_0 and hence k_0.*

2.10 Koutecky-Levich analysis

The Koutecky-Levich analysis models the electric current due to electrochemistry taking in account both the current due to diffusion, i_l and current due to kinetic reaction, i_k. Koutecky-Levich (KL) analysis provides a simple and effective method to extract the electrochemical parameters by excluding the effect due to mass transfer.

Starting with the Butler-Volmer equation,

$$i = i_0 \left(\frac{C_O\left(0\right)}{C_O} e^{-\alpha \frac{F}{RT}(E-E_0)} - \frac{C_R\left(0\right)}{C_R} e^{(1-\alpha)\frac{F}{RT}(E-E_0)} \right), \tag{2.34}$$

where C_O and C_R represent the bulk concentration of oxidant and reductant species respectively, $C\left(0\right)$ is the concentration at electrode surface. Away from the equilibrium potential, consider towards a more electronegative potential $E < E_0$, low $C_R(0)$ and low value of $e^{(1-\alpha)\frac{F}{RT}(E-E_0)}$) in the second term, and higher counter values in the first term, allow use to omit the contribution due to the reductant. So, the second term in Equation 2.34 vanishes, and we are left with,

$$i = i_0 \left(\frac{C_O\left(0\right)}{C_O} e^{-\alpha \frac{F}{RT}(E-E_0)} \right). \tag{2.35}$$

We had already established in Section 2.3, $\frac{C_O(0)}{C_O} = 1 - \frac{i}{i_l}$. So, the expression for current becomes,

$$i = i_0 \left(\left(1 - \frac{i}{i_l} \right) e^{-\alpha \frac{F}{RT}(E-E_0)} \right) \tag{2.36}$$

Dividing by i on both sides and rearranging,

$$\frac{1}{i} = \frac{1}{i_0 e^{-\alpha \frac{F}{RT}(E-E_0)}} + \frac{1}{i_l} \tag{2.37}$$

This can be expressed in compact form as,

$$\frac{1}{i} = \frac{1}{i_k} + \frac{1}{i_l} \tag{2.38}$$

Or in expanded form as,

$$\frac{1}{i} = \frac{1}{i_0 e^{-\alpha \frac{F}{RT}(E-E_0)}} + \frac{1}{0.62nFAD^{\frac{2}{3}}\omega^{\frac{1}{2}}\nu^{-\frac{1}{6}}C} \tag{2.39}$$

This is famously known as Koutecky-Levich equation. A plot of i^{-1} vs $\omega^{-\frac{1}{2}}$ again gives a

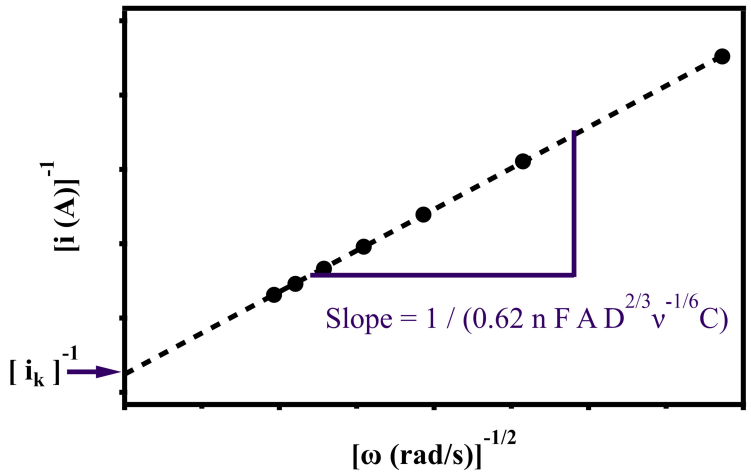


Figure 2.13: *KL plot showing linear relationship between i^{-1} and $\omega^{-\frac{1}{2}}$ for an overpotential at different rotation speeds. The slope can be used to calculate diffusivity and intercept of the trace gives kinetic current, i_k for that overpotential.*

straight line. The slope can be used to determine D whereas the intercept on the y-axis gives the measure of i_k at a given potential E.

2.11 Tafel analysis

After we determine the values of i_k at every potential using the Koutecky-Levich analysis, we can use the expression for i_k for further determination of the kinetic parameters.

$$i_k = i_0 e^{-\alpha \frac{F}{RT}(E-E_0)} \tag{2.40}$$

$$Log(i_k) = Log(i_0) - \alpha \frac{F}{RT}(E - E_0) \tag{2.41}$$

So, again a plot of $Log(i_k)$ vs E is a straight line. This is called a Tafel Plot. As we can see

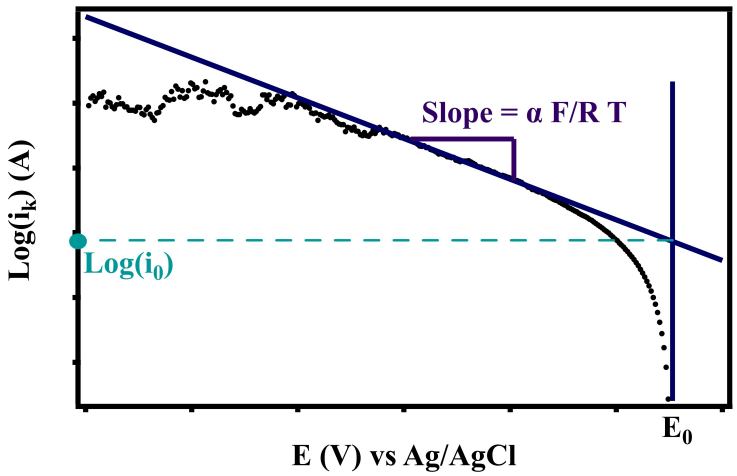


Figure 2.14: *Tafel plot showing a linear section which is unaffected by reverse current at low overpotentials and by miss-limited current at higher potential. Slope of the fitted line is used to measure alpha whereas, the intercept at the equilibrium gives the logarithm of exchange current, $Log(i_0)$, for the system.*

from the expression 2.41, the intercept at the equilibrium potential E_0 gives the logarithm of exchange current i_0. The exchange current is directly related to the standard heterogenous rate constant as $i_0 = nk_0FAC$. With all other parameters known, this gives the value of k_0. Similarly, the slope can be used to find α.

Chapter 3

Diffusivity and kinetic parameters of ferrous/ferric redox reaction in chloride medium

3.1 Introduction

With expansion of renewable sources of energy like solar and wind, redox flow batteries (RFBs) have evolved as promising energy storage systems for cost efficiency and large capacity[9]. Different forms of Ferrous and Ferric ions are used as electrolytes in aqueous redox flow batteries[9] . The ions undergo reduction and oxidation in the electrode-electrolyte interface following the equation below:

$$Fe^{3+}(aq) + e^{-} \underset{k_b}{\overset{k_f}{\rightleftharpoons}} Fe^{2+}(aq)$$

The design and implementation of such RFBs require an accurate account of electron transfer kinetics. Narrowing the studies already done in the past to a relatively well understood electrode - Platinum (Pt), researchers have used methods like faradaic impedance spectroscopy[10], faradaic rectification[11], RDE[12], current-potential curve[13], galvanostatic method[14] to mea-

sure the heterogeneous rate constant, k_0, for the ferrous/ferric ions. The value of heterogeneous rate constant ranges from 1.4×10^{-3} cm s^{-1} [14] to 3.3×10^{-2} cm s^{-1} [11] at room temperature, the range being more than an order in magnitude. To address this variability problem, we have put forward a robust procedure to measure the kinetics using rotating disk electrode. The measurements that we obtain for D and k_0 are reproducible and verifiable with two different analysis approaches and fall within the range of values found in literature.

3.2 Experimental

For the electrochemical system, platinum disk electrode of maximum rotation speed 7000 RPM was purchased from Pine Research (Model AFE2M050PT). The electrode surface was a polycrystalline Pt disk of 5 mm diameter ($A = 0.196$ cm^2), tightly sealed around the circumference by polytetrafluoroethylene (PTFE). The Pine Research MSR Rotator (Model AFMSRCE) was used manually to rotate the working electrode at modulated speeds. A double junction $Ag/AgCl$ reference electrode purchased from Pine Research (Model RREF0024) was used for the entire experiment. A platinum plate was used as a counter electrode.

SP-300 Potentiostat from Biologic was used in conjunction with Biologic EC-Lab Software to manage the entire supply and acquisition of voltages and currents in the electrochemical cell. A jacketed electrochemical cell purchased from Pine Research (Model RRPG310) was used with a circulating water to maintain the temperature of the solution fixed at 298 K.

$FeCl_2.4H_2O$ (CAS 13478-10-9) and $FeCl_3.6H_2O$ (CAS 10025-77-1) were purchased from Fisher Scientific and were used without further purification. 37.7% HCl (CAS 7647-01-01) was purchased from Fisher Scientific. We prepared all solutions using deionized water with resistivity 18 $M\Omega$ cm. A solution of 5 mM of $FeCl_2.4H_2O$ and 5 mM of $FeCl_3.6H_2O$ was prepared. Supporting electrolyte 500 mM HCl was used to increase the conductivity of the solution. This minimizes the iR drop across the cell, and between the WE and RE. The electrolytic solution was purged with argon for around 30 minutes before the beginning of experiment to get rid of the dissolved oxygen. Dissolved oxygen can contribute to the cathodic current by reducing at negative overpotential.

While doing the experiment, a slight roughness or impurity in the electrode can significantly affect the outcome of experiment. The data analysis undergoes several steps and any imperfection in experiment becomes clearly visible in non-linearity of Levich plot, Koutecky-Levich plot and converging anodic and cathodic Tafel plots at a point away from the equilibrium potential. So, good preparation of the electrode as well as electrolyte is crucial to obtain reproducible results. The working electrode was polished before every experiment. We used the electrode polishing kit from Pine Research (Model AKPOLISH). The disk was rubbed in a number 8 pattern on the 0.3 μm alumina slurry onto the microcloth available in the kit for 5 minutes. Then, the electrode was rinsed in DI water and sonicated briefly in acetone, for 30 seconds. As a next step, the electrode was rubbed similarly on the 0.05 μm alumina slurry in a separate microcloth. The electrode was again rinsed in DI water and sonicated in Acetone for 30 seconds. Then it was transferred to DI water for another 30 seconds sonication and rinsed with DI water. The electrode was immersed into the electrolytic solution within 2 minutes of preparing the electrode. We should make sure that there are no air bubbles adhering to the electrode surface after we immerse the electrode into the electrolyte solution. We should be more careful of bubble adhesion on the metal surface.

For the ferrous/ferric system, since it contains both the oxidant and reductant ions in the electrolytic solution, we have two exclusive processes-cathodic and anodic processes to evaluate for the two species. So, cyclic voltammetry was used without rotating the electrode to find out the potential-window around the equilibrium potential to work on.

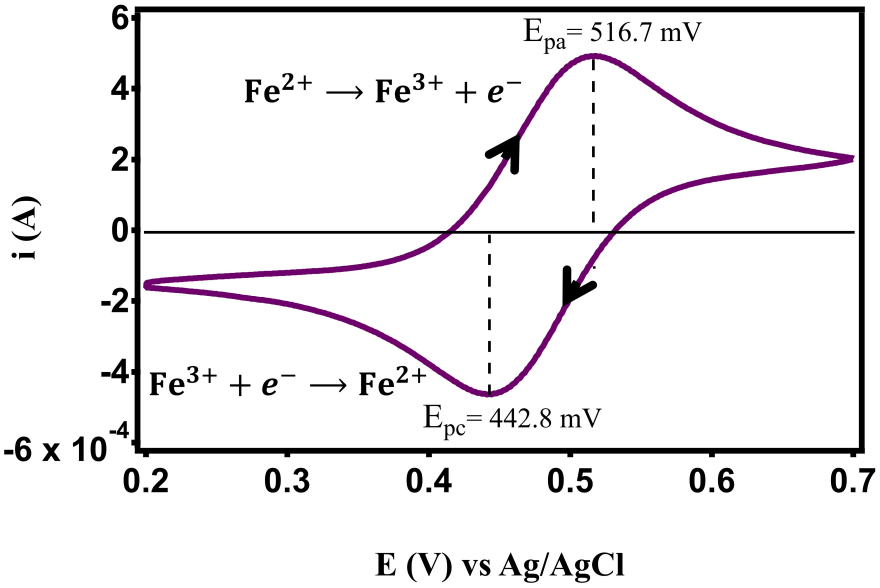


Figure 3.1: *Cyclic voltammogram for the reduction and oxidation from an aqueous solution containing 5mM ferric ion and 5 mM ferrous ion; CV swept back and forth from* $E_1 = 0.7$ V *to* $E_2 = 0.2$ V

We scanned the potential at a rate of 200 $mV\ s^{-1}$. The CV in Figure 3.1 shows a window of potential around $0.2V$ to $0.7V$ to work on. The equilibrium potential was estimated by taking the average of the potentials at peak anodic and cathodic traces, E_{pa} and E_{pc}, which was 0.480 V. We accurately obtained the equilibrium potential by reading the open circuit potential across WE and RE. We found it to be 0.476 V for this particular system at given conditions.

Moving on with the experiment, we got such CVs at different rotation speeds. To reduce the hysteresis and have the least impact of reverse current on the measured current we reduced the scan rate to 5 $mV\ s^{-1}$.

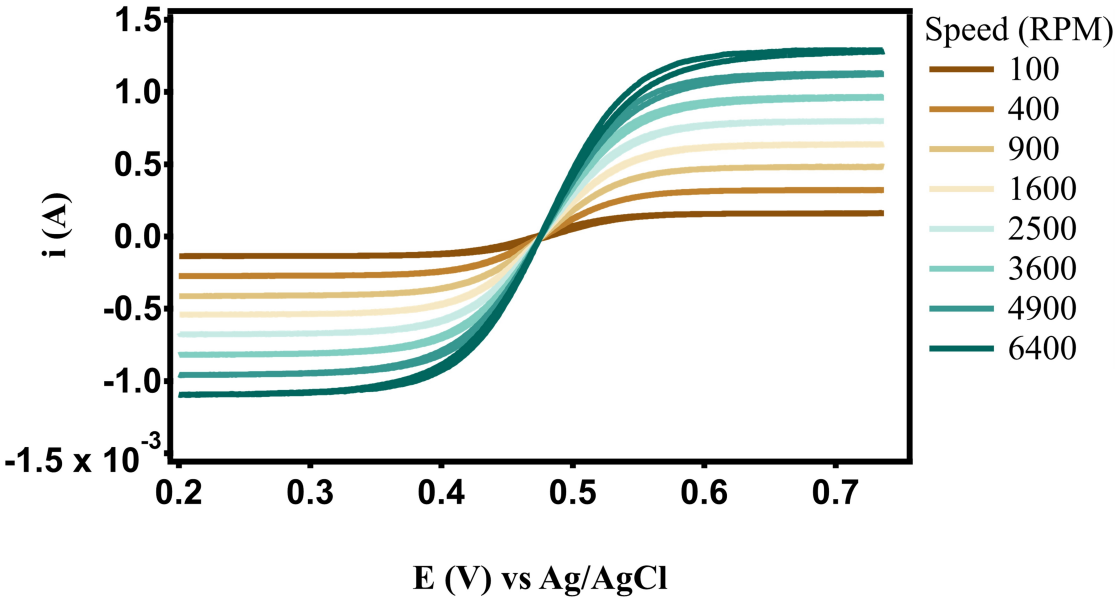


Figure 3.2: *Cyclic voltammogram for the reduction and oxidation from an aqueous solution containing 5mM ferric ion and 5 mM ferrous ion; CV swept back and forth from* $E_1 = 0.75$ *V to* $E_2 = 0.2$ *V; Taken at different rotation speeds ranging from 100 RPM to 6400 RPM*

The rotation speed was selected in the sequence - 100, 900, 2500, 4900, 400, 1600, 3600, 6400 RPM. A non uniform spacing between the traces in the extreme regions would clearly reflect the change in system with time due to external factors like temperature, oxygen dissolution, and impurities.

3.3 Analysis

3.3.1 Levich Analysis

At overpotentials far away from the equilibrium potential, the current is constant and now a function of diffusion. Such diffusion-limited currents are obtained for each rotation speed in both the cathodic and anodic region. Looking at the Levich Equation 2.25,

$$i_l = 0.62nFAD^{\frac{2}{3}}\omega^{\frac{1}{2}}\nu^{-\frac{1}{6}}C,$$

a plot of i_l vs $\omega^{1/2}$ is expected to be a straight line. Figure 3.3 plots the limiting current values vs $\omega^{1/2}$. The dashed lines are linear least squares fits to these data. The lines should pass through the origin as per Equation 2.25. The fitted data in Figure 3.3 demonstrate this.

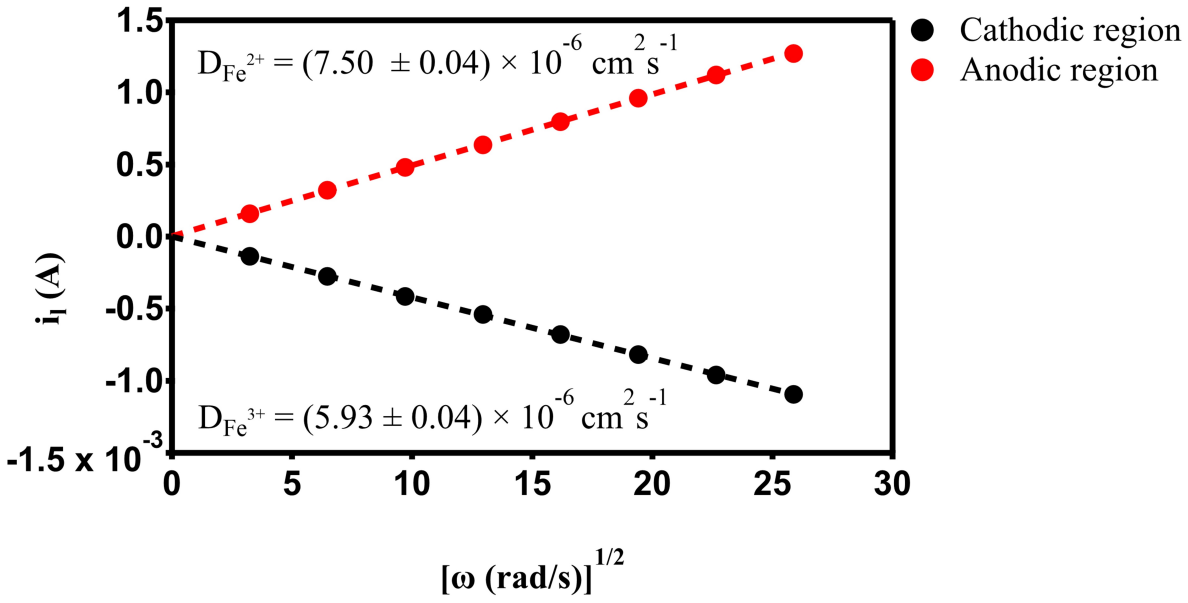


Figure 3.3: *Levich plot showing the value of diffusion-limited currents(dots) at different rotation speeds (100 RPM to 6400 RPM) and fitted to a straight line (dashed line)*

The slopes of these lines, as obtained from the Levich Equation 2.25 are related to the diffusivity as,

$$Slope = 0.62nFAD^{\frac{2}{3}}\nu^{-\frac{1}{6}}C, \tag{3.1}$$

where, $n = 1$, $F = 96485\ C\ mol^{-1}$, $A = 0.196\ cm^2$, $\nu = 0.008917\ cm^2\ s^{-1}$ and $C = 5 \times 10^{-6}$ $mol\ cm^{-3}$. We obtained the values of diffusivity for both oxidant (ferric ion) and reductant (ferrous ion), which are $(7.50 \pm 0.04) \times 10^{-6}\ cm^2\ s^{-1}$ and $(5.93 \pm 0.04) \times 10^{-6}\ cm^2\ s^{-1}$. The uncertainty in these values, $\pm 0.04\ cm^2\ s^{-1}$, is the uncertainty in the slope of the fitting lines as determined by the linear least squares fitting. Lower diffusivity of ferric ions account to higher charge and consequently a higher dielectric drag resistance[15].

3.3.2 Koutecky-Levich Analysis

Koutecky-Levich analysis helps us find the kinetic limited current at different potentials. This is the current that we would have observed under the condition of infinite mass on the electrode surface that are ready to undergo reaction. To do so, we use the Koutecky-Levich equation, 2.39.

At different values of E, the traces of i^{-1} vs $\omega^{-1/2}$ should be straight lines as shown in Figures 3.4 and 3.5.

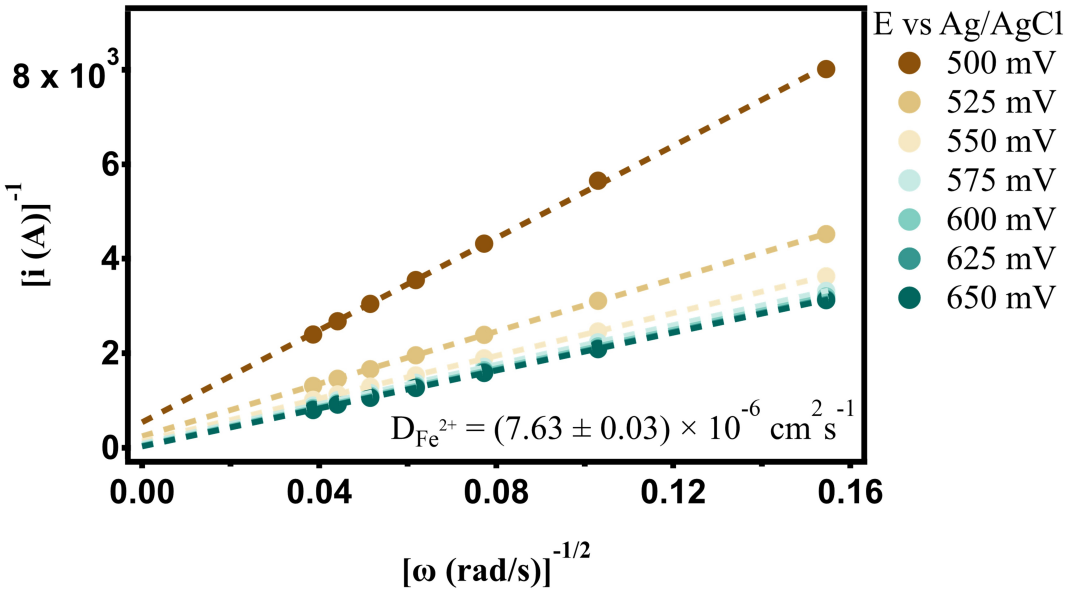


Figure 3.4: *Koutecky-Levich plot for ferrous oxidation at 7 sample potentials in the anodic region; each set of linear dots showing the inverse currents for a potential at different rotation speeds (400 RPM to 6400 RPM) and fitted to a straight line (dashed line)*

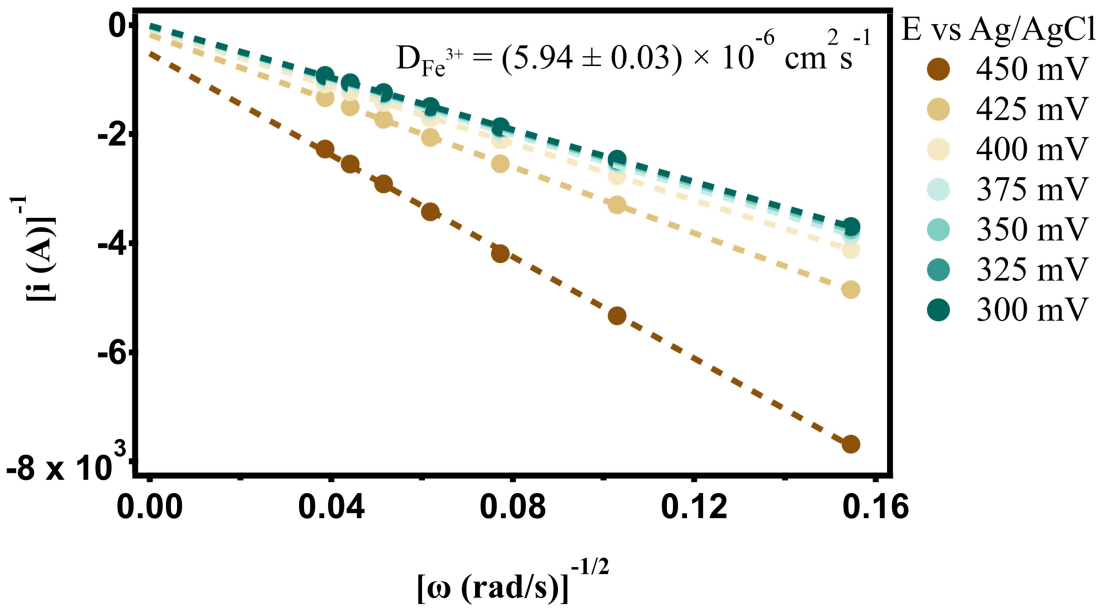


Figure 3.5: *Koutecky-Levich plot for ferric reduction at 7 sample potentials in the cathodic region; each set of linear dots showing the inverse currents for a potential at different rotation speeds (400 RPM to 6400 RPM) and fitted to a straight line (dashed line)*

Looking at the Koutecky-Levich equation again,

$$\frac{1}{i} = \frac{1}{i_0 e^{-\alpha \frac{F}{RT}(E-E_0)}} + \frac{1}{0.62nFAD^{\frac{2}{3}}\omega^{\frac{1}{2}}\nu^{-\frac{1}{6}}C}$$

the equation shows that when $\omega^{1/2}$ is infinite, current measured is equal to the kinetic current. This makes sense considering the fact that at infinite rotation speed, the mass available at the electrode will also be infinite, and there is no limitation due to diffusion. So, extrapolating the lines to $\omega^{-1/2} = 0$ which is $\omega = \infty$, we can find the kinetic current, i_k for every potential. This is the main aim of Koutecky-Levich plot.

In addition to i_k, we also measured the diffusivity using the Koutecky-Levich equation. As we go away from the equilibrium potential, the slope of the lines come to a constant value as shown by parallel traces in the Koutecky-Levich plots - Figures 3.4 and 3.5. This constant slope is related to the diffusivity with the following relation,

$$Slope = \frac{1}{0.62nFAD^{\frac{2}{3}}\nu^{-\frac{1}{6}}C} \tag{3.2}$$

We measured diffusivities using this equation and the values of other parameters as used for Equation 3.1. We found $(7.63 \pm 0.03) \times 10^{-6}\ cm^2\ s^{-1}$ and $(5.94 \pm 0.03) \times 10^{-6}\ cm^2\ s^{-1}$ for ferrous and ferric ions respectively. The uncertainty in these values, $\pm 0.03\ cm^2\ s^{-1}$, is the uncertainty of slope of the fitting lines as determined by the linear least squares fitting.

3.3.3 Tafel Analysis

After we measured the kinetic currents, i_k, at every potential, E, the logarithm of i_k is plotted against E.

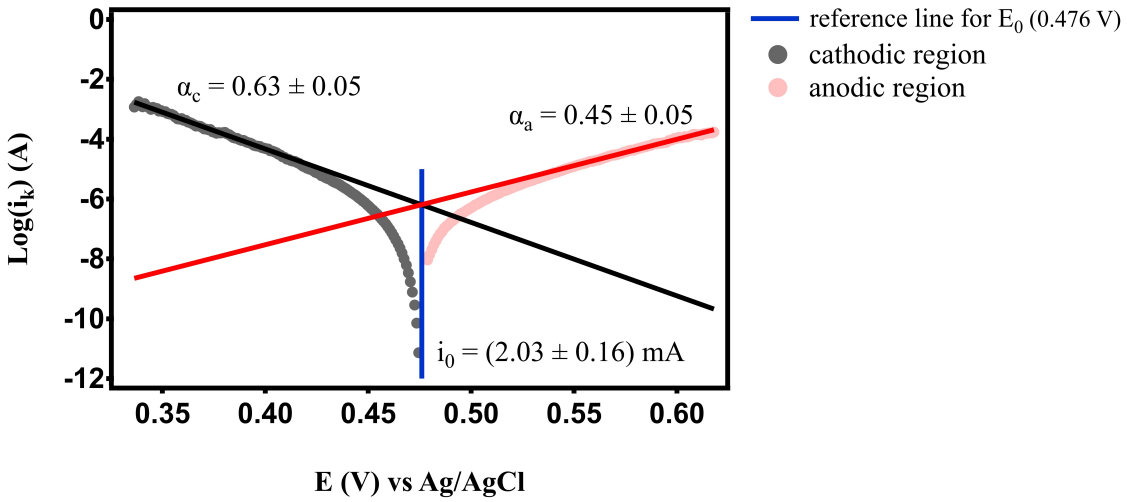


Figure 3.6: *Tafel plot for both oxidation (red) and reduction (black);Dots representing the logarithm of kinetic current at different potentials and the straight lines fitted to the linear section of the Tafel Plot*

Looking at the Equation 2.41,

$$Log(i_k) = Log(i_0) - \alpha \frac{F}{RT}(E - E_0),$$

the Tafel curve should have been a straight line. But, in the region very near to the equilibrium potential, the measured current has an effect of reverse current. So, the current we measure is less than it actually is. That is shown by the decaying curves in the region near the equilibrium potential of $0.476\ V$. So, we select a linear portion of the plot where there

is no effect of reverse current, and the current has not been limited by diffusion. The lines fitted on this region for both anodic and cathodic Tafel curves should intersect at the equilibirum potential, 0.476 mV. This value agrees with our earlier independent measurement of the equilibrium potential.

The value of $Log(i_k)$ at point of intersection is equal to $Log(i_0)$, the logarithm of exchange current, as shown by the Equation 2.41. From this analysis, we obtained the value of i_0, 2.03 $\pm$ 0.16 mA. Using the Equation 2.11 we obtained the value of k_0 using i_0, which is (2.15 $\pm$ 0.17) $\times$ 10^{-2} cm s^{-1}.

Similarly, the slopes multiplied by $\frac{RT}{F}$ should give a measurement of α, which we obtained as $\alpha_c = 0.63 \pm 0.05$ and $\alpha_a = 0.63 \pm 0.05$.

3.3.4 Linearity at low overpotentials

Reducing the Butler Volmer equation for potentials very near to the equillibrium potential, we had reached to Equation 2.33,

$$E - E_0 = i\frac{RT}{F}\left(\frac{1}{i_0} + \frac{1}{i_{lc}} - \frac{1}{i_{la}}\right).$$

The equation shows that i vs E plot should be linear near to the equilibrium potential.

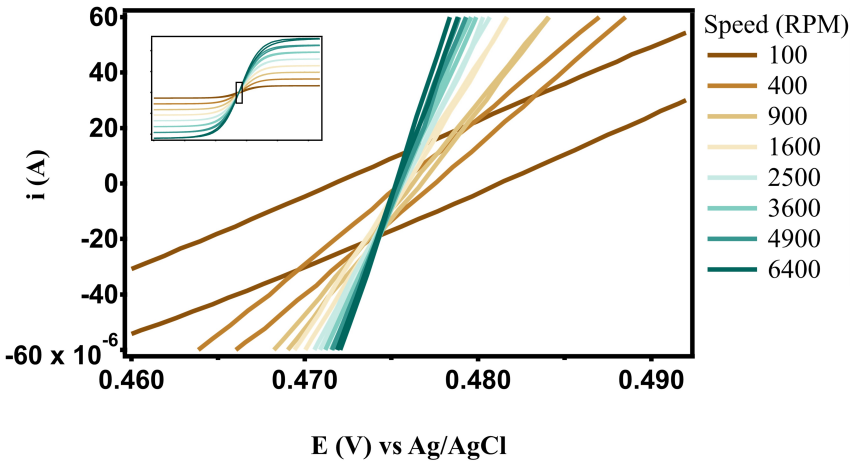


Figure 3.7: *Linearity in IV trace near the equilibrium potential; The slope at equilibrium potential is used to calculate i_0 and ultimately k_0*

An expanded view of CVs shown previously in Figure 3.2 around the equilibrium potential is shown in the Figure 3.7.

Slopes of the traces for each rotation speed were obtained by averaging the slopes of fitted lines along forward and reverse traces, which were nearly equal. The table 3.1 shows the measurement details.

RPM	i_{lc} (A)	i_{la} (A)	Slope$(A\ V^{-1})$	i_0 (A)	j_0 $(A\ cm^{-2})$	k_0 $(cm\ s^{-1})$
100	-1.37×10^{-4}	1.59×10^{-4}	2.76×10^{-3}	2.01×10^{-3}	1.02×10^{-2}	2.12×10^{-2}
400	-2.75×10^{-4}	3.22×10^{-4}	5.33×10^{-3}	1.75×10^{-3}	8.93×10^{-3}	1.85×10^{-2}
900	-4.16×10^{-4}	4.80×10^{-4}	7.79×10^{-3}	1.96×10^{-3}	1.00×10^{-2}	2.07×10^{-2}
1600	-5.41×10^{-4}	6.37×10^{-4}	9.85×10^{-3}	1.87×10^{-3}	9.53×10^{-3}	1.98×10^{-2}
2500	-6.78×10^{-4}	7.98×10^{-4}	1.22×10^{-2}	2.21×10^{-3}	1.13×10^{-2}	2.34×10^{-2}
3600	-8.19×10^{-4}	9.61×10^{-4}	1.40×10^{-2}	1.90×10^{-3}	9.72×10^{-3}	2.01×10^{-2}
4900	-9.59×10^{-4}	1.12×10^{-3}	1.61×10^{-2}	2.09×10^{-3}	1.07×10^{-2}	2.21×10^{-2}
6400	-1.09×10^{-3}	1.27×10^{-3}	1.80×10^{-2}	2.17×10^{-3}	1.11×10^{-2}	2.29×10^{-2}
			Mean	2.00×10^{-3}	1.02×10^{-2}	2.11×10^{-2}
			S. D.	1.47×10^{-4}	7.49×10^{-4}	1.55×10^{-3}

Table 3.1: *Measurement of slope, and calculation using Equation 2.33 for* i_0*, and Equation 2.11 for* j_0 *and* k_0*.*

3.4 Results and conclusion

The linear fit with R^2 values more than 0.9999 for Levich Plot, and Koutecky Levich plot support our procedure for RDE analysis. The linear section of Tafel section is difficult to obtain because of reverse current nearer to equilibrium potential and mass-limitation farther from the equilibrium potential. We were able to obtain that region with high speed rotating disk of upto 6400 RPM. Consequently beautiful conversion of the Tafel plots was seen right at the equilibrium potential reference line.

The diffusivities as measured using Levich analysis were $D_{Fe^{2+}} = 7.5 \times 10^{-6}\ cm^2\ s^{-1}$ and $D_{Fe^{3+}} = 5.93 \times 10^{-6}\ cm^2\ s^{-1}$ for ferrous and ferric ions respectively. The diffusivities measured using Koutecky-Levich analysis were $D_{Fe^{2+}} = 7.63 \times 10^{-6}\ cm^2\ s^{-1}$ and $D_{Fe^{3+}} = 5.94 \times 10^{-6}\ cm^2\ s^{-1}$. Experiment performed by Angell and Dickinson[16] on sulphate system

showed the values of diffusivity to be $D_{Fe^{2+}} = 6.1 \times 10^{-6}\ cm^2\ s^{-1}$ and $D_{Fe^{3+}} = 5.5 \times 10^{-6}\ cm^2\ s^{-1}$. Literature values and two approaches getting us close values support our measurement.

From the Tafel plot, we obtained $\alpha_{red} = 0.63$ and $\alpha_{ox} = 0.45$. The values are self verifiable, meaning the sum of α_{red} and α_{ox} should be 1. Ours add up to 1.08 which is very close to the ideal case. We obtained $k_0 = 2.15 \times 10^{-2}\ cms^{-1}$ from the intercept on the Tafel Plot. Using entirely different section of the CV we calculated k_0 using low overpotential approximation. That led us to $k_0 = 2.11 \times 10^{-2}\ cms^{-1}$ which is shown in table 3.1. Obtaining close values of k_0 using exclusive sections of CV and within the range of values found in literature[10–14] makes us believe that the procedure is robust and gets us accurate values of diffusivity and kinetic parameters. A major strength about this procedure is that, it is verifiable within itself from - the linearity in Levich and Koutecky-Levich plots, the Levich traces passing through the origin, Tafel plots converging to the equilibrium potential, $\alpha_{Fe^{2+}}$ and $\alpha_{Fe^{3+}}$ summing close to 1, and getting same results through independent analysis approaches.

The difficulty in performing this procedure lies in the consistency in the working electrode area. The working electrode requires thorough cleaning and polishing to maintain consistent surface area for every other experiment. The roughness contributes to a larger surface area and surprisingly large value of current can be observed. The impurities adsorbed in the working electrode can lower the surface area of the electrode and current-trend goes on decreasing with time. To tackle these, and verify that there are no such effects in our procedure, we used the alternate rotation speed sequence. The rotating disk that we used is not recommended to work at tempeatures lower than 283 K and higher than 303 K. So, we have a limited range of temperature to work, unless we opt for other rotating disks in the market. Nevertheless, within its scope, this experiment procedure, and analysis technique has proved to be promising for our purpose.

Chapter 4

Diffusivity and kinetic Parameters of silver ions in perchlorate medium

4.1 Introduction

This research was done as part of a larger project of enhancing electrochemical reaction rate using stochastic noise signal. To study the rate of such reactions, it is essential to quantify accurately the kinetics of the reactions. Moreover, the quantification technique should later allow the introduction of stochastic noise so that we can observe the rate amplification through kinetic parameters. Here, we quantify kinetic parameters of silver ion exchange reaction that electrodeposits silver metal at Au working electrode from silver perchlorate aqueous solution.

$$Ag^{+}(aq) + e^{-} \rightleftharpoons Ag(s)$$

This procedure uses rotating disk electrode to measure diffusivity, D, symmetry factor, α, and mainly the heterogeneous reaction rate constant, k_0. This technique later allows easy modification to observe the same parameters in the presence of stochastic noise signal, as an extension to this work.

Several works have been done to determine the kinetic parameters in silver exchange reaction, at Ag electrode in perchlorate medium using galvanostatic method[17;18]; at Ag electrode

in nitrate and thiosulfate medium by means of polarization curve and AC-impedance technique[19]; at Au electrode in perchlorate system using RRDE technique[20]; and at Ag electrode in iodide system using RDE technique[21]. Price and Vermileya[22] used short period IV relation at whiskered Ag electrode in nitrate system. The values of k_0 range from $6 \times 10^{-6} cms^{-1}$ [19] to $3.43 \times 10^{-1} cms^{-1}$ [17] for different working electrodes and media. This huge variability in observation makes it necessary to develop and stick to a consistent procedure and technique to measure the kinetics, and study the effect of stochastic noise in electrodeposition of silver.

4.2 Experimental

The experimental setup is much similar to the one for iron system, as discussed in chapter 3. For the electrochemical system, gold disk electrode of maximum rotation speed 3000 RPM was purchased from Pine Research (Model AFE5T050AU). The electrode surface was a polycrystalline Au disk of 5 mm diameter ($A = 0.196 cm^2$), tightly sealed around the circumference by polytetrafluoroethylene (PTFE). The jacketed electrochemical cell was used to maintain the temperature of the solution fixed at 293 K.

$AgClO_4$ (CAS 7783-93-9) was purchased from Fisher Scientific and used without further purification. 70%-$HClO_4$ (CAS 7601-90-3) was purchased from Sigma Aldrich. A solution of 1 mM of $AgClO_4$ was prepared, with supporting electrolyte 100 mM of $HClO_4$.

The working electrode was polished and used before experiment as described for iron system in section 3.2.

Unlike the ferrous/ferric system, silver system contains only the oxidant ions in the electrolytic solution. So, we have only the cathodic process to evaluate for the oxidant. So, a cyclic voltammetry was obtained without rotating the electrode to find out the potential-window around the equilibrium potential to work on.

We scanned the potential at the rate of 20 $mV\ s^{-1}$. The CV in Figure 4.1 shows a window of potential around $0.1V$ to $0.6V$ to work on. The equilibrium potential was accurately obtained by reading the open circuit potential across WE and RE. It was found to be 0.407 V vs $Ag/AgCl$ reference electrode, for this particular system at given conditions.

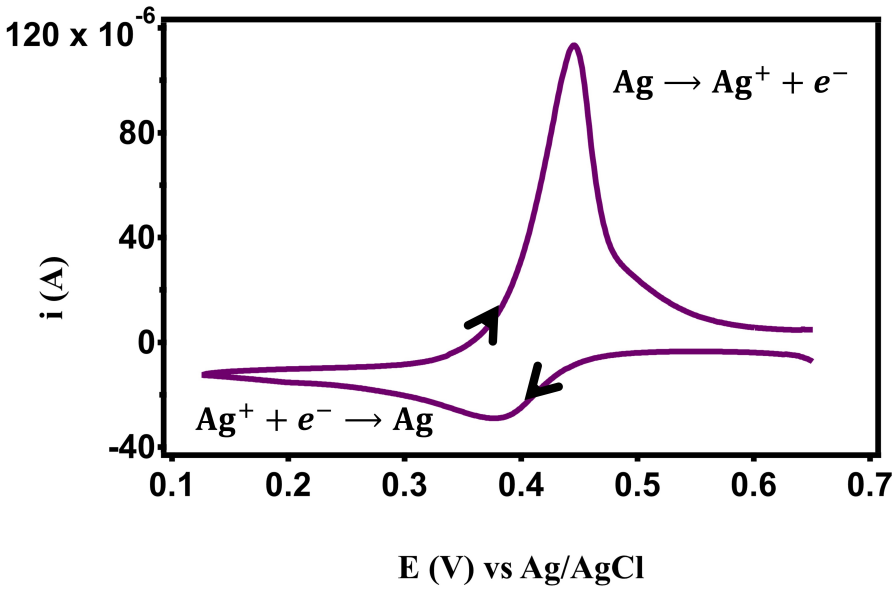


Figure 4.1: *Cyclic voltammogram for the reduction of silver ion from an aqueous solution containing 1mM Silver perchlorate; CV swept back and forth from* $E_1 = 0.65V$ *to* $E_2 = 0.125V$

The CV shows an interesting behavior towards the end of anodic (more positive) region. The CV doesn't meet at the initial starting point, rather a small current still exists (< 10 μA). Since this system involves a true deposition of silver metal on the gold surface, the small current is due to incomplete dissolution of silver metal back to the electrolyte solution. Starting another cycle at this point won't see the same working electrode as was in the earlier cycle. With every cycle, the working electrode surface will be different due to incomplete dissolution of silver. To tackle this problem, the WE was kept at a higer potential, 0.8 V vs $Ag/AgCl$, until the current measured in less than 500 nA. This makes it certain that essentially all the silver has dissolved back into the solution and the working electrode is the same for each cycle.

Since the dissolution was of no concern for kinetic parameter evaluation, we could reduce our task to obtain linear sweep voltammtery for every rotation speeds and later clean the electrode electrochemically. So, we obtained LSVs from 0.65 V to 0.125 V at different rotation speeds at 5 $mV\ s^{-1}$ scan rate.

The rotation speed was selected in the sequence - 100, 400, 900, 1600, 2500, 225, 625, 1225,

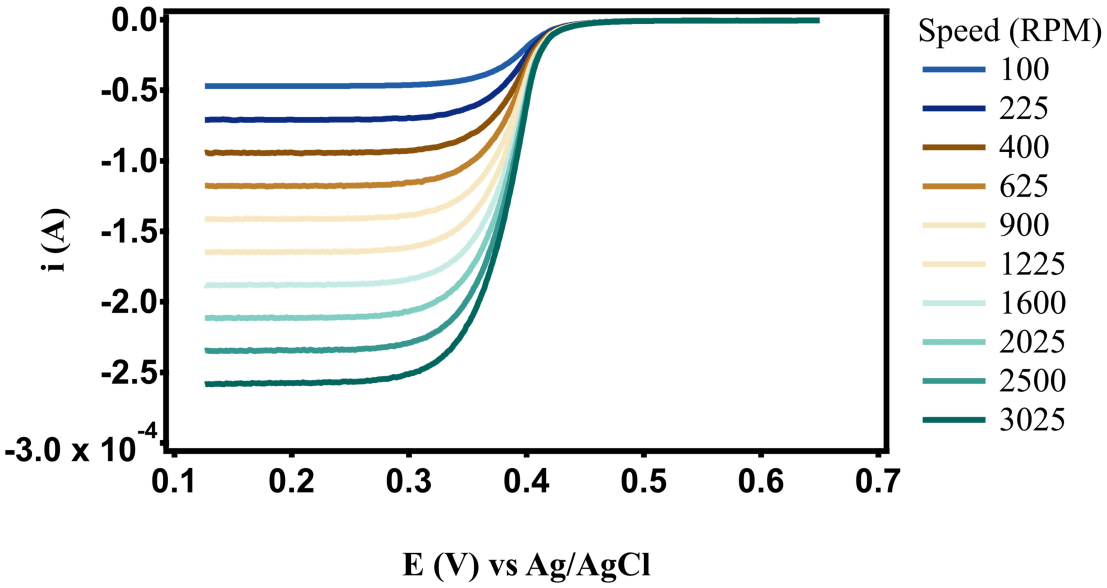


Figure 4.2: *Linear sweep voltammogram for reduction of silver ion from an aqueous solution containing 1mM silver perchlorate and 100 mM perchloric acid; LSV swept from* $E_1 = 0.65V$ *to* $E_2 = 0.125V$ *vs Ag/AgCl; Taken at different rotation speeds ranging from 100 RPM to 3025 RPM*

2025, and 3025 RPM. A non uniform spacing between the current traces in the diffusion-limited region would clearly reflect the change in system with time due to external factors like temperature, oxygen dissolution, and impurities.

4.3 Analysis

4.3.1 Levich Analysis

At potentials far away from the equilibrium potential, the current is constant, a function of diffusion. Such diffusion-limited currents are obtained for each rotation speeds from the CV, Figure 4.1 and plotted against the square root of rotation speed. From the Levich equation 2.25,

$$i_l = 0.62nFAD^{\frac{2}{3}}\omega^{\frac{1}{2}}\nu^{-\frac{1}{6}}C,$$

the plot of i_l vs $\omega^{1/2}$ must be a straight line, as shown in the Levich plot-Figure 4.3. The line is expected to pass through the origin as per Equation 2.25.

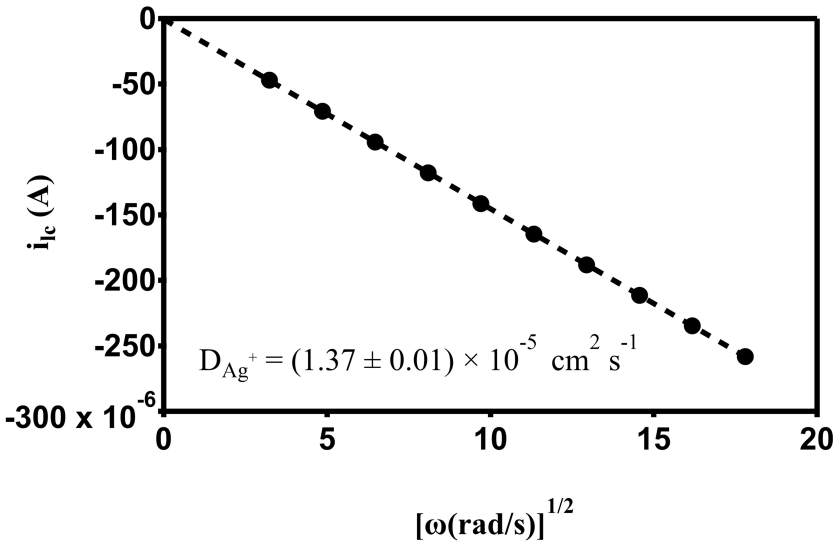


Figure 4.3: *Levich plot showing the value of diffusion-limited currents(dots) at different rotation speeds (100 RPM to 3025 RPM) and fitted to a straight line (dashed line)*

The dashed black line, a linear least squares fit to these data, confirms this expectation. The y-intercept is $(-0.50 \pm 0.15) \times 10^{-6}\ A$. The slope is $(-1.45 \pm 0.01) \times 10^{-5}\ A\ rad^{-1/2}\ s^{1/2}$, where the uncertainty was determined by the least squares fitting routine.

The slope as obtained from the Levich equation 2.25 is related to the diffusivity with Equation 3.1

$$Slope = 0.62nFAD^{\frac{2}{3}}\nu^{-\frac{1}{6}}C,$$

where,$n = 1$, $F = 96485\ C\ mol^{-1}$, $A = 0.196\ cm^2$, $\nu = 0.010023\ cm^2\ s^{-1}$ and $C = 1 \times 10^{-6}\ mol\ cm^{-3}$.

From calculation, we obtained the value of diffusivity for silver ions which is $(1.37 \pm 0.01) \times 10^{-5}\ cm^2\ s^{-1}$.

4.3.2 Koutecky-Levich Analysis

At different values of E, i^{-1} are plotted against $\omega^{-1/2}$ which should be straight lines as indicated by Koutecky-Levich equation 2.39,

$$\frac{1}{i} = \frac{1}{i_0 e^{-\alpha \frac{F}{RT}(E-E_0)}} + \frac{1}{0.62nFAD^{\frac{2}{3}}\omega^{\frac{1}{2}}\nu^{-\frac{1}{6}}C}.$$

Our i^{-1} vs $\omega^{-1/2}$ data are plotted in Figure 4.4. The linear least squares fits to these data

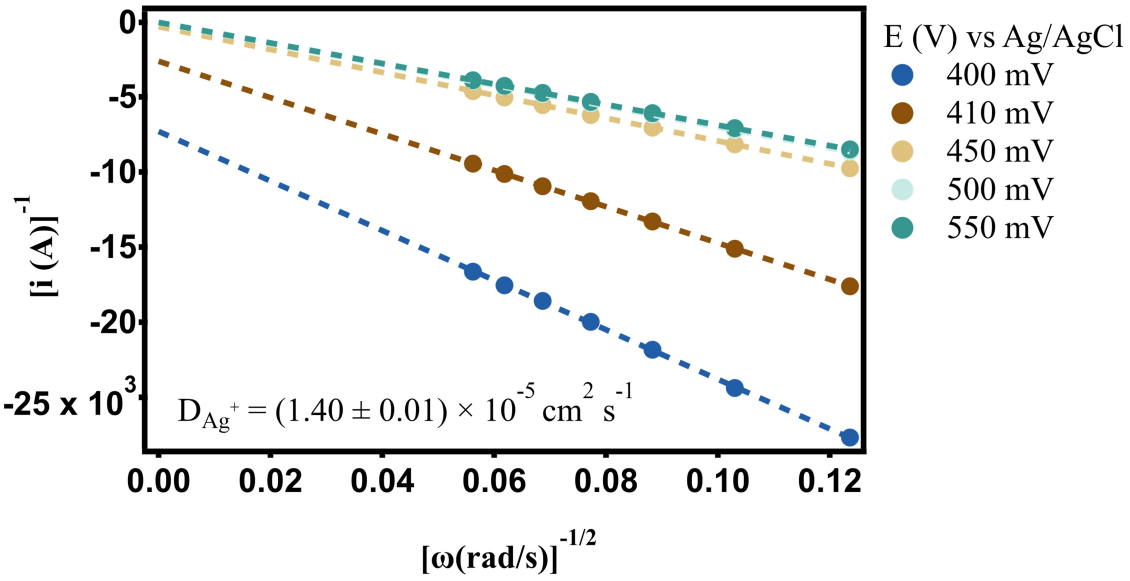


Figure 4.4: *Koutecky-Levich plot for reduction of silver ions for 7 sample potentials; each set of linear dots showing the inverse currents for a potential at different rotation speeds (625 RPM to 6400 RPM) and fitted to a straight line (solid line)*

sets are the dashed lines. The fit quality is good: $R^2 = 0.999994$. Equation 2.39 shows that when $\omega^{1/2}$ is infinite, current measured is equal to the kinetic current. Extrapolating the fitting lines to $\omega^{-1/2} = 0$ which is $\omega = \infty$, we can find the kinetic current, i_k for every potential.

As we go away from the equilibrium potential, the slope of the lines remain constant. This constant slope is related to the diffusivity by Equation 3.2,

$$Slope = \frac{1}{0.62nFAD^{\frac{2}{3}}\nu^{-\frac{1}{6}}C}$$

Using this technique also, we measured the diffusivity for silver ion, which is $(1.40 \pm 0.01) \times 10^{-5}\ cm^2\ s^{-1}$

4.3.3 Tafel Analysis

After we measured the kinetic currents, i_k, at every potential, E, the logarithm of i_k is plotted against E, following Equation 2.41,

$$Log(i_k) = Log(i_0) - \alpha \frac{F}{RT}(E - E_0).$$

The data points are shown by the black dots. We select the linear portion of the plot where

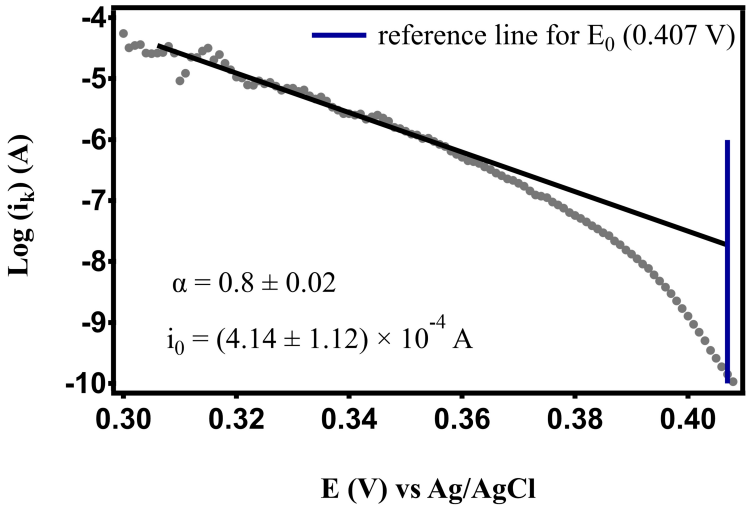


Figure 4.5: *Tafel plot for reduction; Dots representing the logarithm of kinetic current at different potentials and the straight lines fitted to the linear section of the Tafel Plot*

there is no effect of reverse current, and the current has not been limited by diffusion. The linear least squares fits to this portion, is shown by the solid black line. The fit quality is, $R^2 = 0.965$. As per Equation 2.41, the line intersects at the equilibrium potential reference line (where $E = E_0$) to give the $Log(i_0)$, which is $-7.79 \pm 0.27\ A$. This gave us the value of exchange current, $i_0 = (4.14 \pm 1.12) \times 10^{-4}\ A$. Using the Equation 2.11 we obtained the value of k_0 using i_0, which is $(2.18 \pm 0.50) \times 10^{-2}\ cm\ s^{-1}$.

Similarly, the slope of the line is $-32.3 \pm 0.81\ A\ V^{-1}$. The slope multiplied by $\frac{RT}{F}$ should give a measurement of α, which we found, $\alpha = 0.8 \pm 0.02$.

4.4 Results and conclusion

The linear fit with R^2 values more than 0.9999 for Levich Plot, and Koutecky Levich plot support our procedure for RDE analysis. We were able to obtain the linear region in Tafel plot even with relatively slower rotating disk.

The diffusivity measured using Levich analysis was $D = 1.37 \times 10^{-5}\ cm^2\ s^{-1}$ for the silver ions. The diffusivity measured with Koutecky-Levich analysis was $D = 1.40 \times 10^{-5}$ $cm^2\ s^{-1}$. Kraichman and Hogge[23] obtained $D = 1.42 \times 10^{-5} cm^2\ s^{-1}$ for diffusivity of silver ions in nitrate system which is in excellent agreement with our finding. We could not find any literature that measures diffusivity of silver ions in perchlorate system possibly making our measurement to be the first one.

From the Tafel plot, we obtained $\alpha = 0.8$, which is within the range of values found by Despic and Bockris[17] - 0.5 and Ashiru and Farr[21] - 0.84. We obtained $k_0 = 2.18 \times 10^{-2}\ cm$ s^{-1} from the intercept on the Tafel Plot. The value is certainly within the vast range of values available in literature, $6 \times 10^{-6} cm\ s^{-1}$ [19] to $3.43 \times 10^{-1} cm\ s^{-1}$ [17] and most close to values obtained by Bockris[17;18] , 8.26×10^{-3} to $3.43 \times 10^{-1} cm\ s^{-1}$. Thus, we believe that this procedure gives us reasonable values for kinetic parameters and diffusivity, and can be the basis for study with further modifications.

Chapter 5

Development of appropriate system to measure diffusivity of indium ions in acetate medium

5.1 Introduction

Indium has already shown its versatile applicability with metallic (soldering, cryogenics) and semiconductor (integrated circuits, lasers, LEDS) properties over the years. Indium tin oxide (ITO) has been extensively used in flat panel displays, and copper indium galium diselenide (CIGS) in solar cells. Recent developments have seen indium to be useful in Lithium batteries to enhance ultrafast electrochemistry. Li_2ZrCl_6 when doped with In^{3+} ions and combined with Li-In anodes has shown to increase conductivity of the electrolyte, and high initial discharge capacity in solid-state batteries[24]. Practical applications to these sectors require highly refined indium and electrodeposition is the most used technique to do so.

Electrodeposition of indium on glassy carbon and platinum from methanesulfonate solution[25], on dropping mercury electrode from perchlorate solution[26], and again on glassy carbon from tetrabutylammonium chloride[27] solution have been studied in the past. We

have chosen to electrodeposit indium from acetate solution for acetate considered an excellent precursor for production of ultra high purity compounds and nanoscale materials. Diffusion of indium ions across the solution is an important parameter to study for electrodeposition. We studied to find a favorable supporting electrolyte to do so and determined the diffusivity of In^{3+} on aqueous acetate solution. Metallic indium will be deposited onto Au rotating disk electrode at temperatures 283 K and 293 K.

5.2 Experimental

The experimental setup for the electrochemical system for indium is much similar to the silver system - Chapter 4, with the same working electrode, reference electrode and counter electrode. The Pine Research MSR Rotator (Model AFMSRCE) for this system, was controlled by dc supply through Agilent waveform generator 33220A. We built a custom potentiostat to work in a 3-electrode electrochemical system. We used Keithley 2400 sourcemeter to supply voltage to the working electrode through the potentiostat. Keithley 2182A nanovoltmeter was used to measure reference electrode voltage, and current flowing through the system. All these instruments were remotely controlled using Python code, given in Appendix A. The code ran the instruments and generated data files for further analysis.

A jacketed electrochemical cell was used to maintain the temperature of the solution at 283K and 293K for two experiments described in this chapter. $99.99\% - In(CH_3COOH)_3$ (CAS 25114-58-3) was purchased from Sigma Aldrich and used without further purification. We prepared all solutions using deionized water with resistivity $18M\Omega cm$. $99.9\% - CH_3COOH$ (CAS 64-19-7) was purchased from Sigma Aldrich. $87.7\% - KOH$ (CAS 1310-58-3) was purchased from Fisher Scientific. $99.4\% - CH_3COONa$ (CAS 127-09-3) was purchased from Fisher Scientific. The working electrode was polished before every experiment and used in the same way as mentioned for iron system in Section 3.2.

To begin with, a solution of 10 mM of $In(CH_3COO)_3$ was prepared, with supporting electrolyte 500 mM CH_3COOH. The electrolytic solution was purged with Argon for around 30 minutes before the beginning of experiment to get rid of the dissolved oxygen.

The Indium system contains (In^{3+}) in the electrolytic solution as an oxidant lowering our task to study only the cathodic process. We obtained a cyclic voltammogram without rotating the electrode to find out the potential-window around the equilibrium potential to work on.

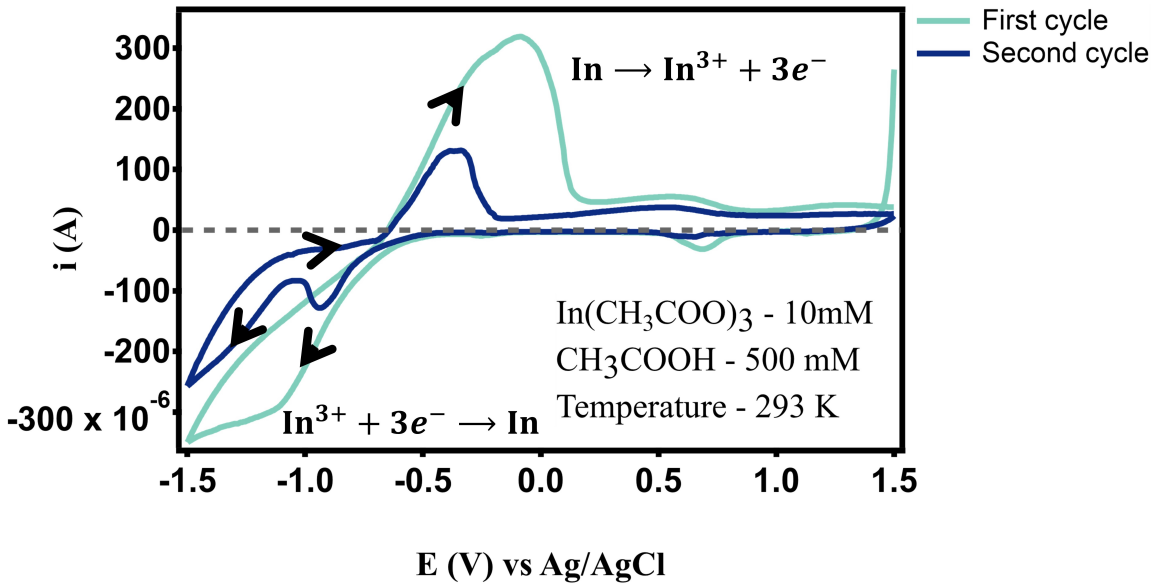


Figure 5.1: *Cyclic voltammogram for the reduction of* In^{3+} *ion, swept back and forth from* $E_1 = 1.5\ V$ *to* $E_2 = -1.5\ V$ *at* $25mVs^{-1}$

The CV showed several problems. It looked in a bad shape with variation in instantly repeated cycle. It shows the reduction of In^{3+} at around $-0.5\ mV$. But there is an another reduction lobe that starts at around $-1.0\ V$. The latter refers to the breakdown of water and evolution of Hydrogen gas. The indium metal was seen heavily deposited on the electrode surface and wasn't possible to fully clean electrochemically which is shown by the continuous positive current on reverse loop in the anodic region.

We tried to take LSV at different rotation speeds for the same solution. Neither the traces were in order of rotation speed which it should have been, nor did they show a proper diffusion-limited region. Water breakdown happening around our focused region was not favorable for study. Moreover, the working electrode was different for each rotation speed because we could never clean off the electrode completely with electrochemistry.

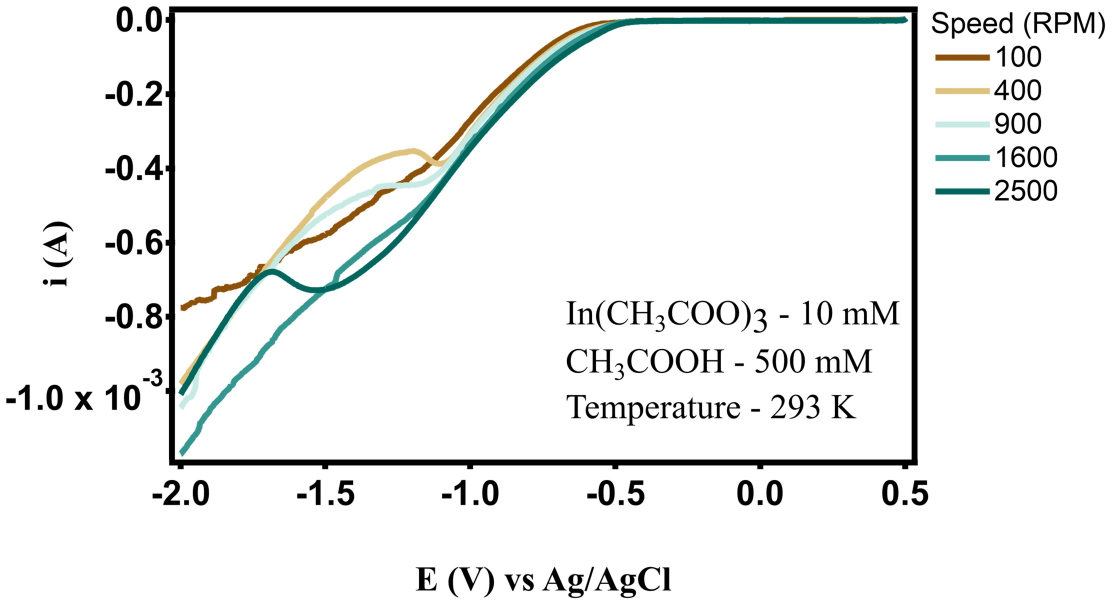


Figure 5.2: *LSV for the reduction of* In^{3+} *ion from* $E_1 = 0.5\ V$ *to* $E_2 = -2\ V$ *at* $10\ mV\ s^{-1}$

As an attempt to solve the problems, after the first run, the electrode was taken out of the system and polished with the $0.05\mu m$ alumina slurry in a microcloth for 5 minutes. It was as usual rinsed with DI water, sonicated in acetone for 30 seconds, sonicated in water for 30 seconds, and again rinsed with fresh DI water. Only then it was put back into the solution for next run. To counter the concentration of H^+ ions and discourage water breakdown, 500 mM of KOH was added to the solution.

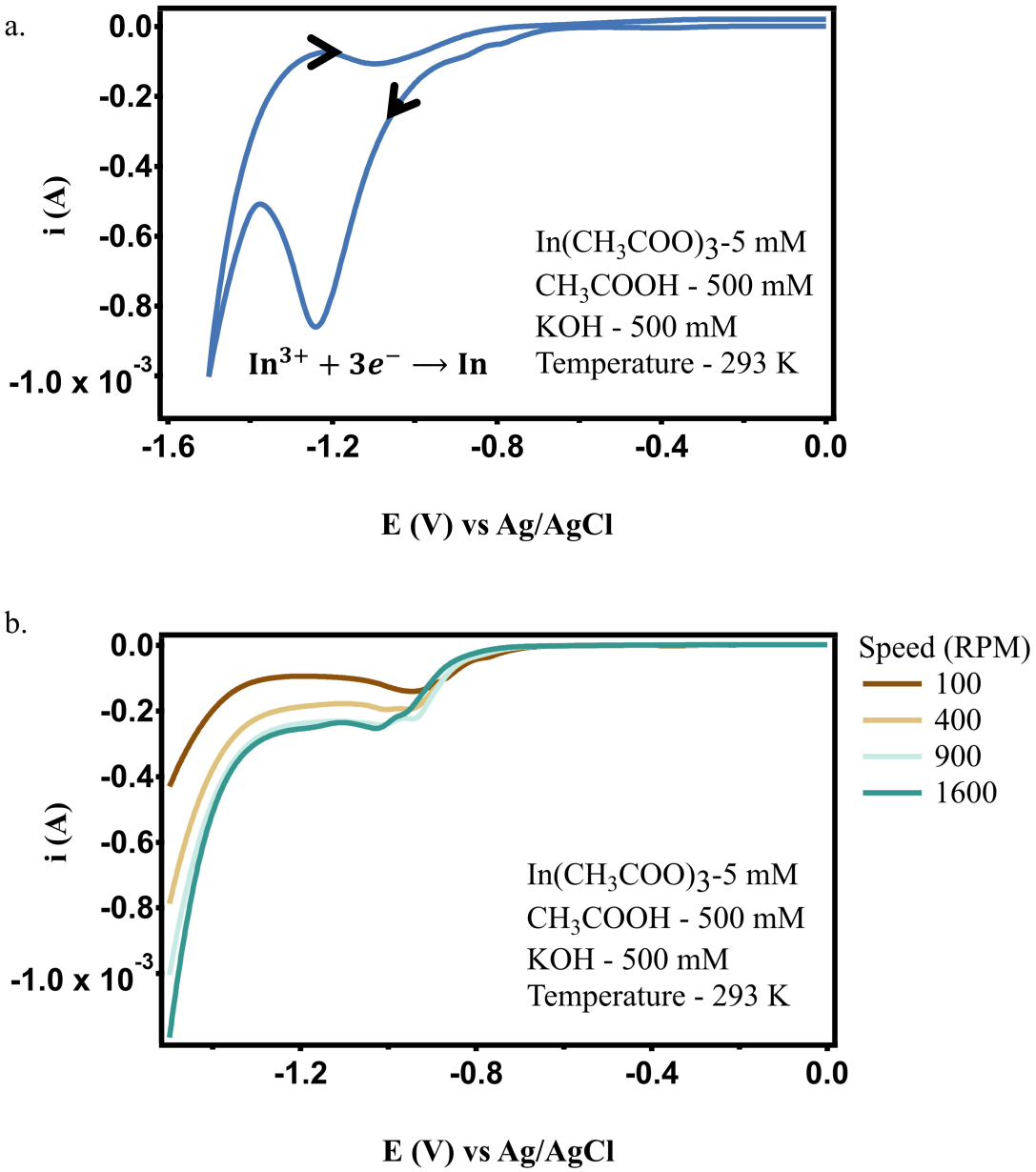


Figure 5.3: ***a.*** *CV for the reduction of* In^{3+} *ion, swept back and forth from* $E_1 = 0\ V$ *to* $E_2 = -1.5\ V$ *at* $25mV\ s^{-1}$*;* ***b.*** *LSV for the reduction of* In^{3+} *ion from* $E_1 = 0\ V$ *to* $E_2 = -1.5\ V$ *at* $10\ mV\ s^{-1}$

The CV and LSV in Figure 5.3 show a push in the onset of water breakdown. The LSV traces show a good diffusion-limited region and are in order according to the rotation speeds, but still lack uniform spacing which is required for a trustworthy Levich plot.

We did a check on the background current due to water and the supporting electrolytes.

We also checked for CH_3COONa to see if it can be a proper substitution, since it does not inhibit water breakdown by lowering the pH.

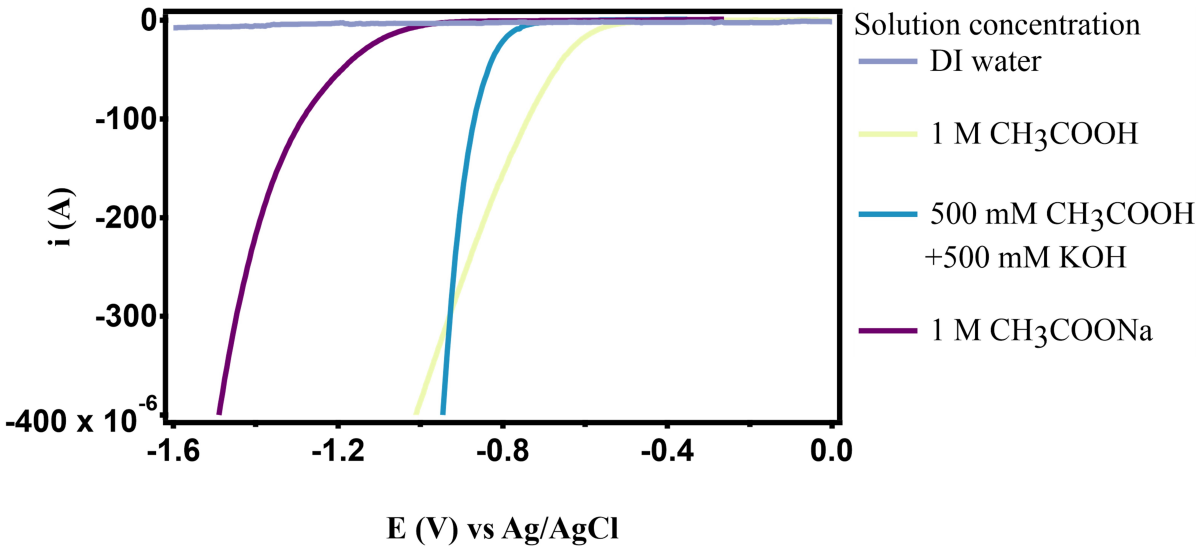


Figure 5.4: *Background current contribution to the measured current, scan rate* - $10mV\ s^{-1}$

The LSV traces show that, for DI water, the breakdown of water begins at around $-1.0\ V$ but it has minimal contribution to the measured current, $< 10\ \mu V$. Reduction begins earliest for CH_3COOH, and CH_3COONa seemed to push the reduction onset the farthest. That gave us a reason to substitute the supporting electrolyte with Sodium acetate.

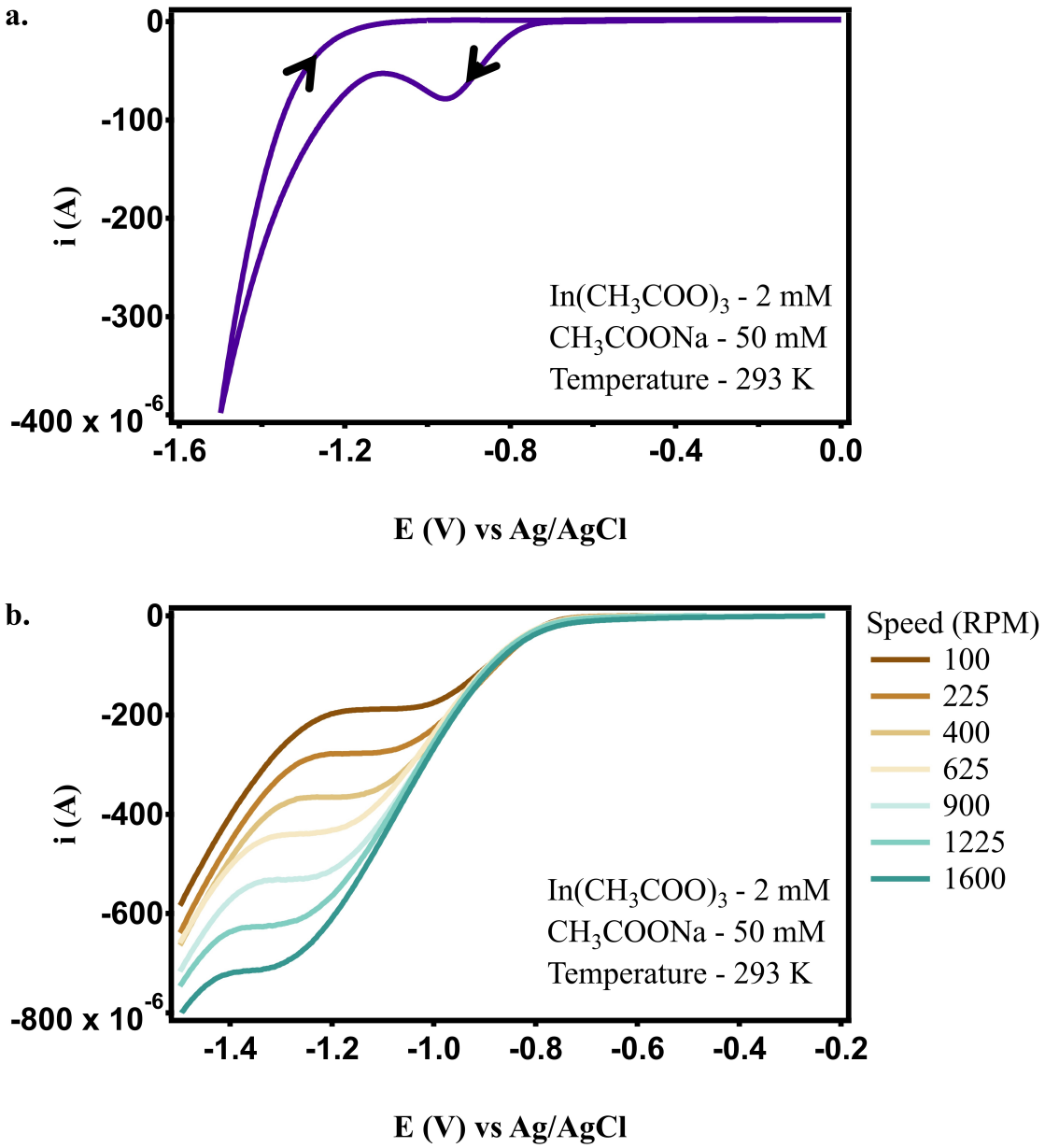


Figure 5.5: ***a.*** *CV for the reduction of* In^{3+} *ion, swept back and forth from* $E_1 = 0\ V$ *to* $E_2 = -1.5\ V$ *at* $25\ mV\ s^{-1}$*;* ***b.*** *LSV for the reduction of* In^{3+}*;* $E_1 = -0.2\ V$ *to* $E_2 = -1.5\ V$ *at* $10mV\ s^{-1}$

The CV and LSV in Figure 5.5 show minimal effect due to the breakdown of water. The LSV traces show a good diffusion-limited region and are in order according to the rotation speeds. The traces are uniformly spaced in that region as expected.

The same experiment was repeated at a lower temperature. The traces show far more push of water breakdown due to lower temperature, which is clearly visible by comparing the 1600 RPM traces in Figures 5.5.b and 5.6.

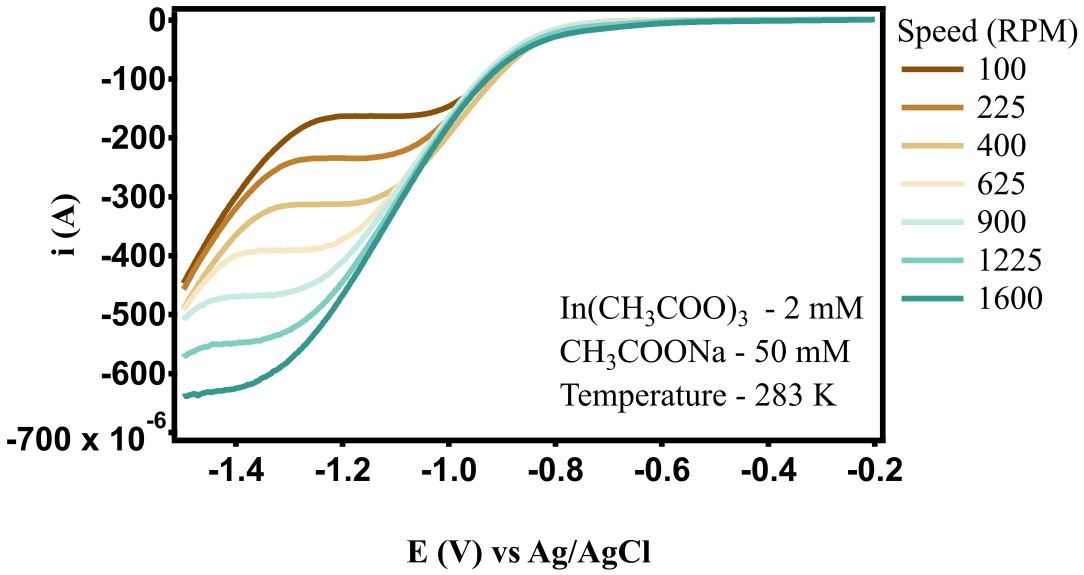


Figure 5.6: *CV for the reduction of* In^{3+} *ion, swept back and forth from* $E_1 = 0\ V$ *to* $E_2 = -1.5\ V$ *at* $25\ mV\ s^{-1}$

5.3 Analysis

5.3.1 Levich Analysis

The diffusion-limited currents were obtained for each rotation speed and plotted against $\omega^{1/2}$ for Levich plot. According to the the Levich equation 2.25,

$$i_l = 0.62nFAD^{\frac{2}{3}}\omega^{\frac{1}{2}}\nu^{-\frac{1}{6}}C,$$

the plot of i_l vs $\omega^{1/2}$ is expected to be a straight line and should pass through the origin. It can be observed from Levich plot-figure 5.7, which shows the linear least squares fit to the data (dashed lines) and extrapolation of the lines to the origin.

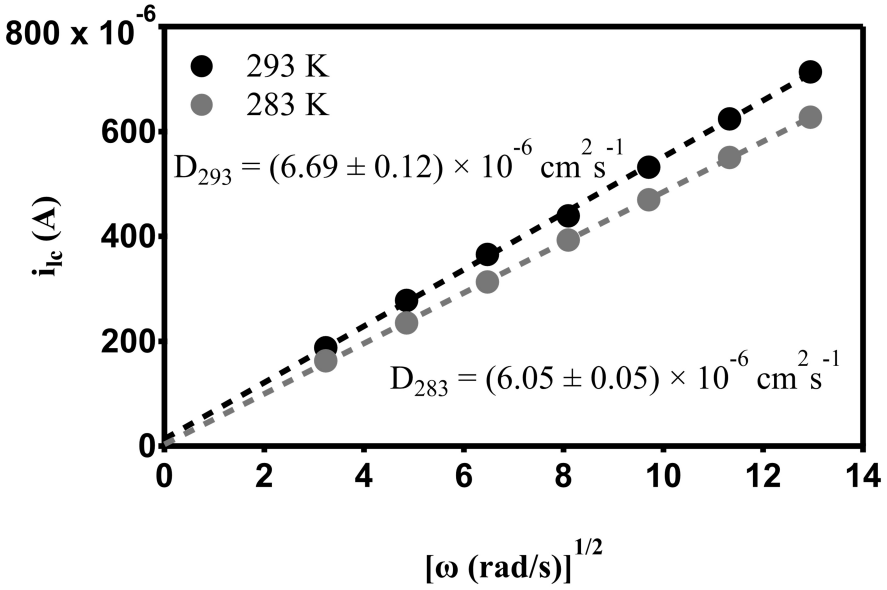


Figure 5.7: *Levich plot showing the values of diffusion-limited currents (dots) at different rotation speeds (100 RPM to 1600 RPM), and fitted to straight lines (dashed) at temperatures 293 K and 283 K*

The slopes of these fitted lines were, $(5.38 \pm 0.06) \times 10^{-5}\ A\ rad^{-1/2}\ s^{1/2}$ and $(4.82 \pm 0.03) \times 10^{-5}\ A\ rad^{-1/2}\ s^{1/2}$ for temperatures 293 K and 283 K respectively. The uncertainties in these slopes were obtained from the linear least squares fitting routine. The slopes are related to the diffusivity according to the Equation 3.1,

$$Slope = 0.62nFAD^{\frac{2}{3}}\nu^{-\frac{1}{6}}C,$$

where, $n = 3$, $F = 96485\ C\ mol^{-1}$, $A = 0.196\ cm^2$, $\nu_{293} = 0.010023\ cm^2\ s^{-1}$, $\nu_{283} = 0.013081\ cm^2\ s^{-1}$ and $C = 2 \times 10^{-6}\ mol\ cm^{-3}$.

Calculating diffusivity using these values in Equation 3.1, we measured, $D_{293} = (6.69 \pm 0.12) \times 10^{-6}\ cm^2\ s^{-1}$ and $D_{283} = (6.05 \pm 0.05) \times 10^{-6}\ cm^2\ s^{-1}$. The R^2 values for the fitted lines were better for the trace at lower temperature, 0.9998 vs 0.9993 possibly because of the slowing down of water breakdown and less impact on current measurement.

5.4 Results and conclusion

We developed a system for studying In^{3+} diffusivity in acetate medium. Sodium acetate seems to be the best supporting electrolyte for indium acetate diffusivity measurments. The linear fits with R^2 values more than 0.999 for Levich plot support our procedure of RDE analysis. The diffusivities measured using Levich analysis were $6.69 \times 10^{-6}\ cm^2\ s^{-1}$ at 293 K and $6.05 \times 10^{-6}\ cm^2\ s^{-1}$ at 283 K. Avchukir[27] obtained $D = 4.41 \times 10^{-6}\ cm^2\ s^{-1}$ using RDE technique and $D = 6.63 \times 10^{-6}\ cm^2\ s^{-1}$ using chronoamperometry, at 298 K in chloride system. Monnens[25] measured $D = 2.2 \times 10^{-6}\ cm^2\ s^{-1}$ in methanesulfonate system using RRDE technique. $D = 9.6 \times 10^{-6}\ cm^2\ s^{-1}$ was measured by Inoye[26] at 300 K in perchlorate system. The literature values are in good agreement with our measurement. Any work that measures diffusivity of In^{3+} ions in acetate system was not found in literature, possibly making this the first study.

For this system, the working electrode is difficult to clean electrochemically. So, it requires us to work more on consistency of working electrode surface. The water breakdown occuring around the area of our interest hampers the current measurement. So, other techniques to shift the breakdown onset at more negative potential should be developed, possibly by increasing the pH of the solution. As a future directive, the system can also be used to study the kinetics of the indium ions at the Au electrode.

Chapter 6

Conclusion and future prospects

We have successfully used rotating disk electrode to measure the diffusivity of three different metal ions - iron (ferrous (Fe^{2+}) and ferric (Fe^{3+})), silver (Ag^{+}) and indium (In^{3+}). The diffusivity was measured in different electrolytic systems - chloride (Cl^{-}), perchlorate (ClO_4^{-}) and acetate (CH_3COOH) respectively. Perchlorate and acetate systems were entirely new media for the silver and indium diffusivity study.

We used a high-speed rotating disk (up to 7000 RPM) for the iron system. The ferric ions showed around 20% lower diffusivity compared to the ferrous ions, possibly because of the higher solvation effect and higher dielectric drag resistance due to the extra charge. We used a relatively lower-speed rotating disk (up to 3000 RPM) for the silver and indium systems. The breakdown of water did not affect the iron and silver system as it did the indium system. That is because of the potential window where indium ions show a reduction. Indium ions start reducing at a much lower potential around ($-0.5\ V$) compared to around ($0.45 - 0.55\ V$) for silver and iron ions.

The rotating disk electrode was able to separate the kinetic region and the diffusion-limited region for all the systems. The iron system reached the diffusion-limited region so early that it was difficult to get a proper kinetic region free of reverse reaction and diffusion limitation. So we had to use the higher speed electrode for the iron system. Lower diffusivity values in order of $10^{-6}\ cm^2\ s^{-1}$ for iron compared to $10^{-5}\ cm^2\ s^{-1}$ for silver justify this

necessity.

Being able to separate a proper kinetic region, we measured the kinetic currents for every working electrode potential. We linearly fitted the Koutecky-Levich plot and extrapolated the lines to obtain the current at an infinite rotation speed. Obtaining a good Koutecky-Levich plot is challenging in this technique. Kinetic currents obtained from not-so-good Koutecky-Levich plots later show up in the Tafel plot with no linear portion to fit on, and with unusual values of α (greater than 1). We obtained reasonable values of α and calculated the heterogeneous rate constants which agree with the literature values.

Having consistency in the working electrode surface is one of the challenges in this technique. This requires a consistent polishing procedure of the disk. Varying temperature or impurities adsorbing on the disk surface may sometimes change the behavior of the system with time. We should be aware of the potential window we are working on, to omit any unnecessary reactions that might occur around that window, such as the water breakdown that we saw in the indium system. Bubbles might appear on the electrode surface, which drastically affects the area of the working electrode, sometimes completely shielding the working electrode from a reaction.

The values that we obtained and the procedure we followed are good bases for further studies with modifications to the system. The iron system showed that the procedure, within its scope is self-verifiable and can be used to measure accurate values of diffusivity and kinetic parameters. With the use of self-built potentiostat and python to remotely sense voltage and current in the indium system, we are in a good position to introduce stochastic noise signals. We can now send stochastic noise to the iron and silver system and measure the kinetic parameters again. It will be interesting to see if the rate increases as we hypothesized. Increasing accuracy for the indium system by possibly increasing the pH of the system, and considering it for kinetic parameter analysis is a way to go. The system adds up another trustworthy base to analyze in the presence of stochastic noise.

Certainly, a higher value of the reaction rate constant will have a huge impact on ongoing electrochemical systems. From batteries to thin-film depositions to chemical synthesis, being able to tune up the reaction rate in these systems is a boon and has irreplaceable space in

modern technology and science.

Bibliography

[1] W. Nernst. Theorie der reaktionsgeschwindigkeit in heterogenen systemen. *Zeitschrift für Physikalische Chemie*, 47U:52–55, 1904. doi: 10.1515/zpch-1904-4704. URL https://doi.org/10.1515/zpch-1904-4704.

[2] W. Nernst and E. S. Merriam. Zur theorie des reststroms (nach versuchen von herrn merriam). *Zeitschrift für Physikalische Chemie*, 53U:235–244, 1905. doi: 10.1515/zpch-1905-5313. URL https://doi.org/10.1515/zpch-1905-5313.

[3] A. Eucken. Die ermittelung der absoluten grösse des diffusionsstromes in bewegten elektrolyten. *Zeitschrift für Elektrochemie und angewandte physikalische Chemie*, 38: 341–345, 1932. doi: 10.1002/bbpc.19320380603. URL https://onlinelibrary.wiley.com/doi/abs/10.1002/bbpc.19320380603.

[4] B.G. Levich. The theory of concentration polarization. *Acta Physiochimica U.R.S.S*, 17:257–307, 1942.

[5] B. Levich. *Physicochemical Hydrodynamics*. Prentice-Hall, 1962.

[6] J. Koutecky and B.G. Levich. The application of the rotating disc electrode to studies of kinetic and catalytic processes. *ZHURNAL FIZICHESKOI KHIMII*, 32(7):1565–1575, 1958. ISSN 0044-4537.

[7] T. V. Kármán. Über laminare und turbulente reibung. *ZAMM - Journal of Applied Mathematics and Mechanics / Zeitschrift für Angewandte Mathematik und Mechanik*, 1:233–252, 1921. doi: https://doi.org/10.1002/zamm.19210010401. URL https://onlinelibrary.wiley.com/doi/abs/10.1002/zamm.19210010401.

[8] A. J. Bard and L. R. Faulkner. *Electrochemical Methods: Fundamentals and Applications*. John Wiley and Sons, second edition, 12 2001.

[9] K. Gong, F. Xu, J. B. Grunewald, X. Ma, Y. Zhao, S. Gu, and Yushan Yan. All-soluble all-iron aqueous redox-flow battery. *ACS Energy Letters*, 1:89–93, 2016. doi: 10.1021/acsenergylett.6b00049. URL https://doi.org/10.1021/acsenergylett.6b00049.

[10] J. E. B. Randles and K. W. Somerton. Kinetics of rapid electrode reactions. part 3.—electron exchange reactions. *Trans. Faraday Soc.*, 48:937–950, 1952. doi: 10.1039/TF9524800937. URL http://dx.doi.org/10.1039/TF9524800937.

[11] H. P. Agarwal. Measurement of transfer coefficient and rate constant at equilibrium of fe2+ (0.002 m) fe3+ (0.002 m), h2so4 (1n)/pt electrode from faradaic rectification. *Journal of Electroanalytical Chemistry (1959)*, 5:236–240, 1963. ISSN 0368-1874. doi: https://doi.org/10.1016/0022-0728(63)80010-8. URL https://www.sciencedirect.com/science/article/pii/0022072863800108.

[12] Z. Galus and R. N. Adams. The investigation of the kinetics of moderately rapid electrode reactions using rotating disk electrodes1. *The Journal of Physical Chemistry*, 67:866–871, 1963. doi: 10.1021/j100798a036. URL https://doi.org/10.1021/j100798a036.

[13] J. Jordan and R. A. Javick. Electrode kinetics by hydrodynamic voltammetry—study of ferrous-ferric, ferrocyanide-ferricyanide and iodide-iodine systems. *Electrochimica Acta*, 6:23–33, 1962. ISSN 0013-4686. doi: https://doi.org/10.1016/0013-4686(62)87021-2. URL https://www.sciencedirect.com/science/article/pii/0013468662870212.

[14] F. C. Anson. Exchange current densities for fe(ii)-fe(iii) solutions in sulfuric acid and perchloric acid. *Analytical Chemistry*, 33:939–942, 1961. doi: 10.1021/ac60175a037. URL https://doi.org/10.1021/ac60175a037.

[15] S. Koneshan, R. M. Lynden-Bell, and J. C. Rasaiah. Friction coefficients of ions in aqueous solution at 25 °c. *Journal of the American Chemical Society*, 120(46):12041–12050, 1998. doi: 10.1021/ja981997x. URL https://doi.org/10.1021/ja981997x.

[16] D.H. Angell and T. Dickinson. The kinetics of the ferrous/ferric and ferro/ferricyanide reactions at platinum and gold electrodes: Part i. kinetics at bare-metal surfaces. *Journal of Electroanalytical Chemistry and Interfacial Electrochemistry*, 35(1):55–72, 1972. ISSN 0022-0728. doi: https://doi.org/10.1016/S0022-0728(72)80294-8. URL https://www.sciencedirect.com/science/article/pii/S0022072872802948.

[17] A. R. Despic and J. O'M. Bockris. Kinetics of the deposition and dissolution of silver. *The Journal of Chemical Physics*, 32(2):389–402, 1960. doi: 10.1063/1.1730706. URL https://doi.org/10.1063/1.1730706.

[18] W. Mehl and J. O'M. Bockris. On the mechanism of electrolytic deposition and dissolution of silver. *Canadian Journal of Chemistry*, 37(1):190–204, 1959. doi: 10.1139/v59-026. URL https://doi.org/10.1139/v59-026.

[19] S. Vandeputte, E. Verboom, A. Hubin, and J. Vereecken. Silver reduction in a thiosulfate plus nitrate solution - study of a ce reaction scheme by means of polarization curves and ac-impedance. *JOURNAL OF ELECTROANALYTICAL CHEMISTRY*, 397(1-2):249–260, NOV 1995. ISSN 0022-0728. doi: 10.1016/0022-0728(95)04124-6. URL https://doi.org/10.1016/0022-0728(95)04124-6.

[20] S. Swathirajan and S. Bruckenstein. Interpretation of the potentiodynamic response during the underpotential deposition of silver on polycrystalline gold. *Journal of Electroanalytical Chemistry and Interfacial Electrochemistry*, 146(1):137–155, 1983. ISSN 0022-0728. doi: https://doi.org/10.1016/S0022-0728(83)80117-X. URL https://www.sciencedirect.com/science/article/pii/S002207288380117X.

[21] O. A. Ashiru and J. P. G. Farr. Kinetics of reduction of silver complexes at a rotating disk electrode. *Journal of The Electrochemical Society*, 139(10):2806–2810, oct 1992. doi: 10.1149/1.2068983. URL https://doi.org/10.1149/1.2068983.

[22] P. B. Price and D. A. Vermilyea. Kinetics of electrodeposition of silver. *The Journal of*

Chemical Physics, 28(4):720–721, 1958. doi: 10.1063/1.1744224. URL https://doi.org/10.1063/1.1744224.

[23] M.B. Kraichman and E.A. Hogge. The limiting current on a rotating disc electrode in silver nitrate-potassium nitrate solutions - the diffusion coefficient of silver ion. *JOURNAL OF PHYSICAL CHEMISTRY*, 59(9):986–987, 1955. ISSN 0022-3654. doi: 10.1021/j150531a041. URL https://doi.org/10.1021/j150531a041.

[24] S. Chen, C. Yu, S. Chen, L. Peng, C. Liao, C. Wei, Z. Wu, S Cheng, and J. Xie. Enabling ultrafast lithium-ion conductivity of li2zrcl6 by indium doping. *Chinese Chemical Letters*, 2021. ISSN 1001-8417. doi: https://doi.org/10.1016/j.cclet.2021.12.048. URL https://www.sciencedirect.com/science/article/pii/S1001841721011074.

[25] W. Monnens, C. Deferm, K. Binnemans, and J. Fransaer. Indium electrodeposition from indium(iii) methanesulfonate in dmso. *Phys. Chem. Chem. Phys.*, 22:24526–24534, 2020. doi: 10.1039/D0CP03277H. URL http://dx.doi.org/10.1039/D0CP03277H.

[26] I. Senkichi and I. Hideo. Electrode kinetics of indium (iii) at the dropping mercury electrode. *Bulletin of the Chemical Society of Japan*, 33:149–152, 1960.

[27] K. Avchukir, N. Yessaly, and B. Burkitbayeva. Electrodeposition of indium on glassy carbon from tetrabutylammonium chloride containing solutions. *Eurasian Chemico-Technological Journal*, 21(2):157–163, Jun. 2019. doi: 10.18321/ectj826. URL https://ect-journal.kz/index.php/ectj/article/view/826.

Appendix A

Python code to run electrode rotator, take CV and take LSV for Indium system

```
# -*- coding: utf-8 -*-
"""
Created on Thu Feb 18 12:20:19 2021
Rotating Disk Electrode for Indium System
@author: Shital Babu Rijal
"""

import time
import pyvisa
import numpy as np
from numpy import savetxt
import sys
import winsound

#Directory in the computer to store data files
BaseDirectory = 'C:/Data/sbrijal'

# Feedback resistance in the potentiostat (Ohm)
FR=502

#Creating arrays to save the data
currents=[] #to save current
wpotentials=[] #to save working electrode potential
spotentials=[] #to save supplied potential; supposed to be equal to wpotential
times=[] #to record the real time
LSV=[] #List of rotation speeds for LSV

#Parameters for the beep alert sound
frequency = 2500  #Set Frequency To 2500 Hertz
duration = 1000  #Set Duration To 1000 ms == 1 second
RPMList = {0, 100, 400, 900, 1600, 2500} #Rotation speeds set for RDE

rm = pyvisa.ResourceManager()

#Setting up the RDE Controller
#Address for 33220A Agilent Waveform generator
RDEControl = rm.open_resource('USB0::2391::1031::MY44041466::INSTR')
RDEControl.write(':OUTP:LOAD INF')
RDEControl.write(':SOUR:FUNC DC')

#Setting up the voltmeter which measures feedback current with Channel 1
#and reference electrode potential with Channel 2
#Address for Keithley 2182A nanovoltmeter
voltmeter = rm.open_resource('GPIB0::8::INSTR')
voltmeter.write(":*RST") # resetting the voltmeter

#Defining a module that measures voltage across the
#feedback resistor in current follower of potentiostat
def channel1():
  voltmeter.write(":SENS:CHAN 1")
  voltmeter.write(":SENS:FUNC 'VOLT'")
  voltmeter.write(':SENS:VOLT:NPLC 1')
  voltmeter.write(":VOLT:DC:RANG 10")  # Range for nanovoltmeter

#Defining a module that measures voltage at the
#reference electrode of potentiostat
def channel2():
```

```
  voltmeter.write(":SENS:CHAN 2")
  voltmeter.write(":SENS:FUNC 'VOLT'")
  voltmeter.write(':SENS:VOLT:NPLC 1')
  voltmeter.write(":VOLT:DC:RANG 1")  # Range for nanovoltmeter

#Reads the voltage at the voltmeter
def nanoread():
  voltmeter.write(':READ?')

#Setting up the Sourcemeter which supplies direct voltage for a CV, LSV
#or fixed DC for cleaning electrode
sourcemeter = rm.open_resource("GPIB::24") #Address for 2400 sourcemeter
sourcemeter.write("*rst; status:preset; *cls")
sourcemeter.write(":SENS:CURR:PROT 1")
sourcemeter.write(":SENS:CURR:RANG 1")
sourcemeter.write(":OUTP OFF")
sourcemeter.write(":SOUR:VOLT 0")

#Defining a module to take Linear sweep voltammogram
def applyLSV():
    print('Starting LSV for %d RPM...' %RPM)
    winsound.Beep(frequency, duration)
    Query = input("Did you clean the electrode for taking LSV at %d RPM: " %RPM)
    if Query == 'y':
        print('LSV for %d RPM started.' %RPM)
        sourcemeter.write(":OUTP ON")
        T=time.time()
        for E in np.arange (0, -1.5, -.002):

            tdata=time.time()-T

            sourcemeter.write(":SOUR:VOLT %f" %E)

            channel2()
            nanoread()
            ewe = -float(voltmeter.read())

            channel1()
            nanoread()
            i = float(voltmeter.read())/FR

            currents.append(i)
            wpotentials.append(ewe)
            spotentials.append(E)
            times.append(tdata)

        savetxt('%s/LSV_%d RPM_%s.csv' %(BaseDirectory, RPM, time.strftime("%H%M%S")),\
                np.transpose([wpotentials,currents,spotentials,times]),\
                    header = 'V_%d_%s, I_%d_%s, voltages_%d, times_%d'\
                        % (RPM, time.strftime("%m%d%H%M%S"), \
                           RPM, time.strftime("%m%d%H%M%S"), RPM, RPM),\
                            fmt='%1.9f',delimiter=",", comments='')
        print ('LSV data for %d RPM saved successfully' %RPM)
        del currents[:]
        del wpotentials[:]
        del spotentials[:]
        del times[:]
```

```
    if(Query !='y'):
        print('Invalid entry. Terminating...')
        Exit()

def applyCV():
    print('Starting CV...')
    winsound.Beep(frequency, duration)
    Query = input("Did you clean the electrode for taking CV?")
    if Query == 'y':
        print('CV started...')
        #Input parameters for CV
        E2=-1.5
        E1=.5
        T=time.time()
        scanrate=.002
        for j in range(1): #Number of cycles
            for i in [-1,1]:
                for E in np.arange(E1, E2, scanrate*i):

                    tdata = time.time()-T

                    sourcemeter.write(":SOUR:VOLT %f "%E)

                    channel1()
                    nanoread()
                    i = float(voltmeter.read())/FR

                    channel2()
                    nanoread()
                    ewe = -float(voltmeter.read())

                    currents.append(i)
                    wpotentials.append(ewe)
                    spotentials.append(E)
                    times.append(tdata)

                E2,E1=E1,E2 #To reverse the loop

        savetxt('%s/CV_%d RPM_%s.csv' %(BaseDirectory, RPM, time.strftime("%H%M%S")),\
                np.transpose([wpotentials, currents, spotentials, times]),\
                    header = 'V_%d_%s, I_%d_%s, voltages_%d, times_%d'\
                        % (RPM, time.strftime("%m%d%H%M%S"),\
                           RPM, time.strftime("%m%d%H%M%S"), RPM, RPM),\
                        fmt='%1.9f',delimiter=",", comments='')
        print ('CV data saved successfully.')
        del currents[:]
        del wpotentials[:]
        del spotentials[:]
        del times[:]
    if(Query !='y'):
        print('Invalid entry. Terminating...')
        Exit()

def Exit():

    sourcemeter.write(":OUTP OFF")
```

```
    RDEControl.write(":OUTP OFF")
    sys.exit()

for RPM in RPMList:

    RPMmv=RPM/1000
    RDEControl.write(':SOUR:VOLT:OFFS %f' %RPMmv)
    RDEControl.write(':OUTP ON')

    if RPM==0:
        applyCV()
    if RPM!=0:
        applyLSV()

print("Experiment Complete.")
Exit()
```